

EFFECT OF POLYPHOSPHORIC ACID ON AGING CHARACTERISTICS  
OF PG 64-22 ASPHALT BINDER

Naresh Baboo Ramasamy, B.S.

Thesis Prepared for the Degree of  
MASTER OF SCIENCE

UNIVERSITY OF NORTH TEXAS

December 2010

APPROVED:

Seifollah Nasrazadani, Major Professor  
Cheng Yu, Committee Member  
Haifeng Zhang, Committee Member  
Mike Kozak, Program Coordinator  
Richard Reidy, Interim Chair of the  
Department of Engineering  
Technology  
James D. Meernik, Acting Dean of the  
Robert B. Toulouse School of  
Graduate Studies

Ramasamy, Naresh Baboo. Effect of Polyphosphoric Acid on Aging Characteristics of PG 64-22 Asphalt Binder. Master of Science (Engineering Systems), December 2010, 72 pp., 7 tables, 46 figures, 49 references.

This research presents the results on an experimental investigation to identify the effect of polyphosphoric acid (PPA) on aging characteristics of an asphalt binder. Addition of PPA to asphalt binders is said to improve performance of flexible pavements. Asphalt binder PG 64-22 in modified and unmodified conditions was subjected to aging in the laboratory using a regular oven and also simulated short term aging using rolling thin film oven (RTFO) test. Aging experiments were conducted to analyze the extent of oxidation in terms of changes in molecular structure of the asphalt binder. These changes were appraised using Fourier transform infrared (FTIR) spectroscopy, dynamic shear rheometer (DSR), and epifluorescence microscopy tests. FTIR was used to determine the changes in major bands with addition of PPA. Stiffness and viscoelastic behaviors of asphalts were determined from the DSR test. The stiffness is measured by calculating the shear modulus,  $G^*$  and the viscoelastic behavior is measured by calculating the phase angle,  $\text{Sin } \delta$ . Epifluorescence microscopy is a tool used to study properties of organic or inorganic substances. The morphological characteristics of PPA modified asphalt samples were observed through an epifluorescence microscopy. Epifluorescence microscopy reveals the polymer phase distribution in the asphalt binders. Results of this investigation show PPA addition to asphalt binders improve  $G^*/\text{Sin } \delta$  characteristics of asphalt binders. In addition, presence of PPA in polymer containing asphalt did not adversely affect aging of the binders.

Copyright 2010

by

Naresh Baboo Ramasamy

## ACKNOWLEDGEMENTS

I would like to express my gratitude towards Dr. Seifollah Nasrazadani, my major professor, for his invaluable guidance, encouragement, and support throughout my education and research. I would like to extend my gratitude to the members of my graduate committee members, Dr. Cheng Yu, and Dr. Haifeng Zhang, for their assistance and support at all levels of this thesis project. I would especially like to thank Mr. Jean Valeria Martin from Innophos and Mr. Bill O'Leary for their guidance in asphalt making and for providing the asphalt binders. My appreciation is extended to Mr. Richard Williammee Jr. and Mr. Jerry Peterson of TxDOT for arrangements of RTFO and DSR testing.

The vital support and encouragement of my family during my master's program and research was essential for completing this step in my education. I would especially like to acknowledge my parents, Mr. and Mrs. Ramasamy for their constant moral and financial support.

Last but not least, I would like to thank all my friends who assisted me in completing this thesis dissertation. Special thanks is offered to Dr. Lon Turnbull from the Department of Biological Sciences here at the University of North Texas for extending his help on using the epifluorescence microscopy. On a personal note, I would also like to express my gratitude to Roshini Surendran for her confidence and never ending support. She instigated the self-confidence in me which is the memory of success.

## TABLE OF CONTENTS

	Page
ACKNOWLEDGEMENTS.....	iii
LIST OF TABLES.....	vii
LIST OF FIGURES.....	viii
LIST OF ABBREVIATIONS AND ACRONYMS.....	xi
Chapters	
1. INTRODUCTION.....	1
1.1 Overview.....	1
1.2 Types of Asphalt Pavement Failures and Causes.....	2
1.2.1 Reflective Cracks.....	2
1.2.2 Alligator Cracks.....	3
1.2.3 Transverse Cracks.....	4
1.2.4 Block Cracks.....	4
1.2.5 Longitudinal Cracks.....	5
1.2.6 Slippage Cracks.....	6
1.2.7 Rutting.....	6
1.2.8 Shoving.....	7
1.2.9 Potholes.....	8
1.2.10 Raveling.....	8
1.2.11 Flushing.....	9
1.2.12 Polishing.....	10
1.3 Background.....	11
1.3.1 Asphalt.....	11
1.3.2 Asphalt Manufacturing.....	12
1.3.3 Asphalt Aging.....	14

1.3.4	Polyphosphoric Acid (PPA).....	15
1.3.5	Asphalt Grading System .....	16
1.4	Purpose of Research.....	17
1.5	Research Questions.....	17
2.	LITERATURE REVIEW .....	19
3.	EXPERIMENTAL PROCEDURES.....	29
3.1	Aging.....	30
3.2	Regular Oven Test .....	30
3.2.1	Sample Preparation .....	30
3.3	Rolling Thin Film Oven (RTFO).....	31
3.3.1	Theory.....	31
3.3.2	Sample Preparation .....	32
3.4	Analytical Techniques to be Utilized.....	32
3.5	Fourier Transform Infrared Spectroscopy (FTIR) .....	33
3.5.1	Theory.....	33
3.5.2	Sample Preparation .....	34
3.6	Dynamic Shear Rheometer (DSR).....	36
3.6.1	Theory.....	36
3.6.2	Sample Preparation .....	37
3.7	Epifluorescence Microscopy.....	38
3.7.1	Theory.....	38
3.7.2	Sample Preparations.....	39
3.8	Design of Experiments (DOE).....	40
3.8.1	Aging Protocols .....	41
4.	RESULTS AND DISCUSSIONS.....	42
4.1	Dynamic Shear Rheometer Results .....	42
4.2	Aging Analysis Using FTIR Spectroscopy.....	48
4.2.1	Aliphatic Groups.....	49
4.2.2	CH <sub>3</sub> and –CH <sub>2</sub> Stretching Absorptions .....	50
4.2.3	CH <sub>3</sub> Deformation Absorptions.....	50

4.2.4	CH <sub>3</sub> Deformation Absorption Band Splitting.....	51
4.3	Effect of RTFO Aging on CH <sub>3</sub> and CH <sub>2</sub> Proportions.....	52
4.4	Aging Characterization by Carbonyl Band.....	53
4.5	Epifluorescence Microscopy.....	57
4.5.1	Epifluorescence Microscopy of RTFO Aged Samples.....	58
4.5.2	Epifluorescence Microscopy of Regular Oven Aged Samples.....	60
5.	CONCLUSION.....	66
	REFERENCES .....	68

## LIST OF TABLES

Table 1: Research groups who worked on PPA addition to base binders. ....	27
Table 2: Analysis matrix table for PPA-asphalt interaction study.....	31
Table 3: Effective sizes for each magnification.....	40
Table 4: Asphalt samples used for this research.....	40
Table 5: Asphalt samples kept for 3 weeks .....	41
Table 6: DSR results of RTFO aged asphalt samples.....	43
Table 7: Results of CH <sub>3</sub> and CH <sub>2</sub> .....	52



## LIST OF FIGURES

Figure 1: Flexible pavement typical layers .....	1
Figure 2: Reflective cracks .....	3
Figure 3: Alligator cracks with pothole .....	3
Figure 4: Transverse crack.....	4
Figure 5: Block cracking.....	5
Figure 6: Longitudinal wheel path cracking .....	5
Figure 7: Slippage cracks.....	6
Figure 8: Rutting.....	7
Figure 9: Shoving.....	7
Figure 10: Potholes .....	8
Figure 11: Surface raveling of an asphalt pavement.....	9
Figure 12: Bleeding asphalt .....	9
Figure 13: Polishing.....	10
Figure 14: Schematic of asphalt production in a petroleum refinery.....	14
Figure 15: PPA multifarious structure .....	15
Figure 16: PPA (H <sub>3</sub> PO <sub>4</sub> ) chain.....	16
Figure 17: PG 64-22 asphalt binder .....	17
Figure 18: Rolling thin film oven test.....	32
Figure 19: Schematic of FTIR apparatus .....	34
Figure 20: Measurement of the area of the carbonyl band .....	35

Figure 21: FTIR spectrum of a PG 64-22 + 3% PPA asphalt.....	36
Figure 22: Image of dynamic shear rheometer .....	37
Figure 23: DSR plate setup.....	38
Figure 24: Epifluorescence microscopy.....	39
Figure 25: Plots of shear stress ( $\tau$ ) vs time (a) and shear strain ( $\gamma$ ) vs time (b) for hypothetical asphalt binder .....	43
Figure 26: Comparison of $G^*/\sin \delta$ , KPa vs. PPA containing asphalt.....	44
Figure 27: Comparison of $G^*/\sin \delta$ , KPa for 2% SBS polymer added asphalt compared to neat binder PG 64-22 .....	45
Figure 28: Comparison of $G^*/\sin \delta$ , KPa for synergistic effects of PPA (1-3%) containing 2% SBS asphalt.....	45
Figure 29: Plot of correlation between viscous and elastic behavior of asphalt binders..	46
Figure 30: $G^*/\sin \delta$ for PPA containing neat binder without polymer. ....	47
Figure 31: Plot of $G^*/\sin \delta$ vs. PPA concentration polymer containing PG 64-22 binder .....	47
Figure 32: FTIR spectra of polyphosphoric acid (a) and PG 64-22 asphalt binder (b). ...	49
Figure 33: $\text{CH}_3$ and $-\text{CH}_2$ stretching absorptions.....	50
Figure 34: $\text{CH}_3$ deformation absorptions .....	51
Figure 35: $\text{CH}_3$ deformation absorption band splitting.....	51
Figure 36: Overlay of FTIR spectra comparing PPA containing and base asphalt binders. ....	53

Figure 37: Comparison of FTIR spectra for aged (a) and unaged (b) PPA containing asphalt binders .....	54
Figure 38: Results of area ratio for carbonyl band to CH <sub>2</sub> +CH <sub>3</sub> bands for different asphalt samples.....	55
Figure 39: Change in I <sub>co</sub> for different asphalt binders due to aging as measured by FTIR. ....	56
Figure 40: Difference between PG 64-22 + 2% SBS + 0.1% S and PG 64-22 asphalt binder .....	57
Figure 41: Epifluorescence images of base asphalt (a), 1% PPA added (b), 2% PPA added (c), and 3% PPA added (d). ....	59
Figure 42: Epifluorescence images of PG 64-22 + 2% SBS + 0.1% S (a), PG 64-22 + 2% SBS + 0.1% S + 1% PPA (b), PG 64-22 + 2% SBS + 0.1% S + 2% PPA (c), and PG 64-22 + 2% SBS + 0.1% S + 3% PPA (d). ....	60
Figure 43: Epifluorescence images of PG 64-22 samples containing 2% SBS + 0.1% S	62
Figure 44: Epifluorescence images of PG 64-22 containing 2% SBS + 0.1% S + 1% PPA .....	63
Figure 45: Epifluorescence images of PG 64-22 containing 2% SBS + 0.1% S + 2% PPA .....	64
Figure 46: Epifluorescence images of PG 64-22 containing 2% SBS + 0.1% S + 3% PPA .....	65

## LIST OF ABBREVIATIONS AND ACRONYMS

DSR – Dynamic shear rheometer

FTIR – Fourier transform infrared

PG – Performance grade

PPA – Polyphosphoric acid

RTFO – Rolling thin-film oven

SBS – Styrene butadiene styrene

HMA – Hot mix asphalt

PCC – Portland cement concrete

MSCR – Multiple stress creep recovery

SBR – Styrene butadiene rubber

# CHAPTER 1

## INTRODUCTION

### 1.1 Overview

Over 96% of the world's pavement network is surfaced with asphalt (NCAT, 1999). There are two main types of road pavements, rigid road pavement, and flexible road pavement. The rigid type is surfaced by Portland cement concrete (PCC). Flexible road pavements, which are surfaced with asphalt materials, will be the focus of this work. The reason for being called "flexible" is because the total pavement structure "deflects" due to traffic loads (Arika et al. 2009). A flexible pavement structure is generally composed of several layers of materials (Figure 1). Each layer receives the loads from the above layer, spreads them out, and then passes on these loads to the next layer below (Arika et al. 2009).



Figure 1: Flexible pavement typical layers  
Courtesy: Arika et al. 2009

Every year, approximately \$68 billion is spent on U.S. roadways; half for capital outlays and another half for maintenance activities (Glover, 2007). Lately, a large

percentage of roads in the U.S have been reported to be in poor conditions. There are four major categories of common asphalt pavement surface distress (Donald et al. 1987, 1989, 2002), and the most common causes of each:

1. Cracks
  - a. Transverse, reflective, slippage, longitudinal, block, and alligator cracks.
2. Surface deformation
  - a. Rutting, and shoving.
3. Patches and potholes
4. Surface defects
  - a. Raveling, flushing, polishing.

## 1.2 Types of Asphalt Pavement Failures and Causes

### 1.2.1 Reflective Cracks

Reflective cracks form in an asphalt overlay directly over cracks in the core pavement. This type of failure is caused by horizontal expansion due to temperature changes in the core pavement and also vertical movements due to traffic loads. They are especially noticeable in asphalt overlays on Portland cement concrete pavements. Figure 2 shows a series of reflective cracks.



Figure 2: Reflective cracks  
Courtesy: Kearney et al. 2004

### 1.2.2 Alligator Cracks

Alligator crack (Figure 3) is a series of joined cracks that look like an alligator skin. Typically, these cracks are caused by repeated large deflections of asphalt pavement under heavy traffic load. This type of crack pattern usually indicates that the pavement base was water saturated, poor quality or aging of asphalt in the mix that makes it brittle, high moisture content, and poor drainage below the pavement.



Figure 3: Alligator cracks with pothole  
Courtesy: Kearney et al. 2004

### 1.2.3 Transverse Cracks

Transverse cracks (Figure 4) are perpendicular to the road centerline and are caused by low temperature contraction of the pavement, initiated at the surface, and down into the pavement. As the temperature falls, it contracts the pavement. This causes the inability of asphalt binder to discharge the stresses and thus it cracks.



Figure 4: Transverse crack  
Courtesy: Kearney et al. 2004

### 1.2.4 Block Cracks

In the case of block cracks (Figure 5), the pavement splits into rectangular pieces. The pieces range in size from almost one-foot to ten-foot square. It is more common on low volume roads and on huge paved areas (parking lots). Since these pavements are normally not as well compacted as major roads, higher air voids are a suspected cause.





Figure 5: Block cracking  
Courtesy: Kearney et al. 2004

#### 1.2.5 Longitudinal Cracks

One of the most common one is longitudinal cracks between the wheel paths (Figure 6) and is attributed to a certain popular brand of paver (Kearney et al. 2004). Separation occurs where the two paver slat conveyors drop the HMA in front of the paver augers (Kearney et al. 2004). Longitudinal cracks in the wheel path are usually related to load amount and can lead to alligator cracking.



Figure 6: Longitudinal wheel path cracking  
Courtesy: Kearney et al. 2004

### 1.2.6 Slippage Cracks

Semicircular shaped cracks are referred to as slippage cracks (Figure 7). They are a result from traffic-induced horizontal forces. These cracks are caused by a shortage of a bond between the surface layer and the course below. This shortage of bond may be due to dusts, dirt, oil, or lack of a tack coat.



Figure 7: Slippage cracks  
Courtesy: Kearney et al. 2004

### 1.2.7 Rutting

Rutting is displacement of material, creating channels in wheel paths (Figure 8). It is caused by traffic compaction or displacement of unstable material. Severe rutting on numerous sections of the interstate highway system during the late 1970s and early 80s was one of the main causes for the federal government initiating the \$300 million strategic highway research program (Kearney et al. 2004).



Figure 8: Rutting  
Courtesy: Donald et al. 1987, 1989, 2002

#### 1.2.8 Shoving

Shoving is a form of plastic deformation that results in ripples across the pavement surface (Figure 9). They typically occur when there is severe horizontal stress where traffic starts and stops, at intersections, and on sharp horizontal curves (Kearney et al. 2004).



Figure 9: Shoving  
Courtesy: Kearney et al. 2004

### 1.2.9 Potholes

Potholes are referred to as “bowl shaped” holes as a result from localized breakdown under traffic (Figure 10). The common causes are poor soils, poor drainage, asphalt surface too thin, and poor compaction and pavement maintenance.



Figure 10: Potholes  
Courtesy: Kearney, E.J. et al. 2004

### 1.2.10 Raveling

Raveling is also known as weathering. It is the progressive loss of aggregate from the pavement surface (Figure 11). Raveling is enhanced in the wheel paths by traffic. High air voids in HMA due to late season paving, and also too little asphalt or overheating of the asphalt in the HMA are all typical causes of raveling.



Figure 11: Surface raveling of an asphalt pavement  
Courtesy: Kearney et al. 2004

#### 1.2.11 Flushing

When asphalt rises to the pavement surface, it is called flushing, sometimes referred to as bleeding. This results in a smooth and shiny pavement (Figure 12) that is sticky in hot weather. Some of the most common causes of flushing are loss of stone cover in a chip seal, excessively rich asphalt mixes, and over compaction of a tender HMA mix by heavy traffic (Kearney et al. 2004). A flushed surface is very smooth and is very slippery.



Figure 12: Bleeding asphalt  
Courtesy: Kearney et al. 2004

### 1.2.12 Polishing

Polishing (Figure 13) is a smooth slippery surface caused by traffic wearing off sharp edges of aggregates (Donald et al. 1987, 1989, 2002).

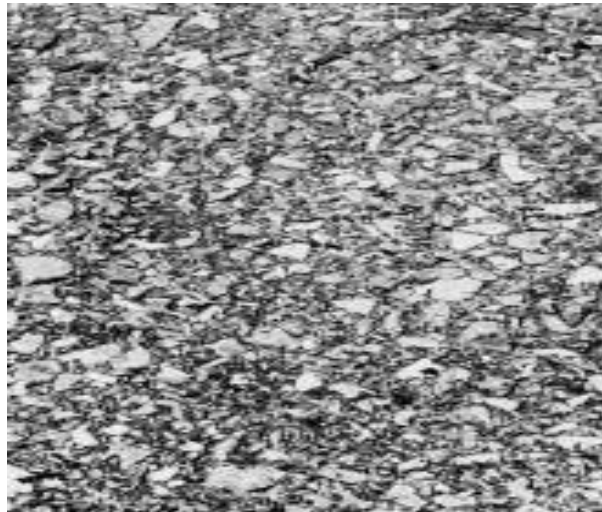


Figure 13: Polishing  
Courtesy: Donald et al. 1987, 1989, 2002

According to the above description, most pavement distresses such as rutting, and cracks are caused by one common factor, which is aging. A chemical process in which the chemical compound mixes with oxygen is known to be oxidation (Herrington et al. 1996). Complete oxidation of asphalt hydrocarbons will generate carbon dioxide and water. Oxygen will attack the specific points on the asphalt molecule where the chemical bond is weak (Herrington et al. 1996). Before beginning to advance construction processes, it is vital to understand the critical behavior and properties of the roads (Glover, 2007). The modification of asphalt to improve performance of pavements has been a challenge and application of polyphosphoric acid (PPA) is used for asphalt improvement. The use of acids to modify asphalt binders dates back to 1939 (Burke et al. 1939). According to Alexander (1973), PPA is a modifier that is used to increase the

viscosity of binders. It has also been reported that PPA can improve the aging resistance of binders (De Filippis et al. 1995). However, the mechanism of PPA modified asphalt binders is still unclear and unknown.

### 1.3 Background

#### 1.3.1 Asphalt

Asphalt is a heavy, dark brown to black inorganic substance, in which the leading constituents are bitumens. The chemical and engineering news (Freemantle, 1999) defines asphalts as highly complex and not well-characterized materials comprising saturated and unsaturated aliphatic (compounds not containing aromatic rings) and aromatic (benzene ring containing) compounds with up to 150 carbon atoms. The basis of crude oil plays a big role in determining asphalt composition. It differs for different basis of crude oil. Oxygen, nitrogen, sulfur, and other heteroatoms are the most common compounds. Asphalt typically contains about 80% by weight of carbon, around 10% hydrogen, fewer than 6% sulfur (S), small amounts of oxygen and nitrogen, and trace amounts of metals such as iron, nickel, and vanadium (Freemantle, 1999).

Based on their solubility in hexane or heptane, the compounds are categorized as asphaltenes or maltenes. Asphaltenes are defined as high molecular weight species that are insoluble in these solvents, while maltenes are soluble and have lower molecular weights. Asphalts normally contain between 5 and 25% by weight of asphaltenes.

The beauty of asphalt is that it is a thermoplastic material. This enables it to soften and harden when heated or cooled. Asphalt is also viscoelastic within a certain

temperature range. It reveals the mechanical characteristics of viscous flow and elastic deformation (Freemantle, 1999).

### 1.3.2 Asphalt Manufacturing

Petroleum, a liquid bitumen is the raw material used in asphalt manufacturing. Asphalt is a natural component of petroleum and there are crude oils which are almost entirely asphalt. The crude petroleum is supplied to oil refineries by the oil wells in order for separation into various fractions and this is done through a process called distillation. Once separation is complete, the components are further refined into various other products including paraffin, asphalt, kerosene, gasoline, naphtha, and diesel oil. Asphalt does not evaporate during the distillation process since it is the base constituent of crude petroleum.

The refining process starts by piping the crude petroleum from a storage tank into a heat exchanger where its temperature is rapidly raised for initial distillation. Then, it goes through an atmospheric distillation tower. Here the light and volatile elements of the crude petroleum are removed through a sequence of condensers and coolers. It is then separated for further refining into gasoline (considered a "light" distillate), kerosene (considered a "medium" distillate), diesel oil (considered a "heavy" distillate), and many other useful petroleum products (Stacey et al. 2006). The end product after this process is so-called topped crude, which is further refined to make asphalt. Vacuum distillation may eliminate sufficient high boiling elements to produce what is called "straight run" asphalt. On the other hand, if the topped crude has enough low volatile constituents which cannot



be economically removed through distillation, solvent de-asphalting may be required to produce asphalt cement of the preferred consistency.

Next, asphalt can be 'cut back' or blended with a volatile substance which results in a product that is soft and effective at a lower temperature than pure asphalt cement. Asphalt refining also involves a process known as emulsifying where asphalt cement is emulsified to produce a liquid that can be easily pumped through pipes, be able to mix easily with aggregate, or sprayed through nozzles.

Powdered asphalt may also be produced by asphalt pulverization. The asphalt is crushed and passed through a series of fine mesh filters to ensure uniform size of the granules. Road oil and aggregate can be mixed with powdered asphalt for construction of pavements. The pressure and heat from the road slowly combines the powder with the aggregate and oil, thus hardening it similarly to asphalt cement. The asphalt may be air blown if the asphalt is to be used for a purpose other than paving, such as roofing, pipe coating, or as a water-proofing material.

This process produces a material that softens at a higher temperature. The asphalt is heated to a temperature of 500°F (260°C) and then air is bubbled through it for one to 4.5 hours. The asphalt remains liquid when cooled. Figure 14 shows the schematic of asphalt production in a petroleum refinery.

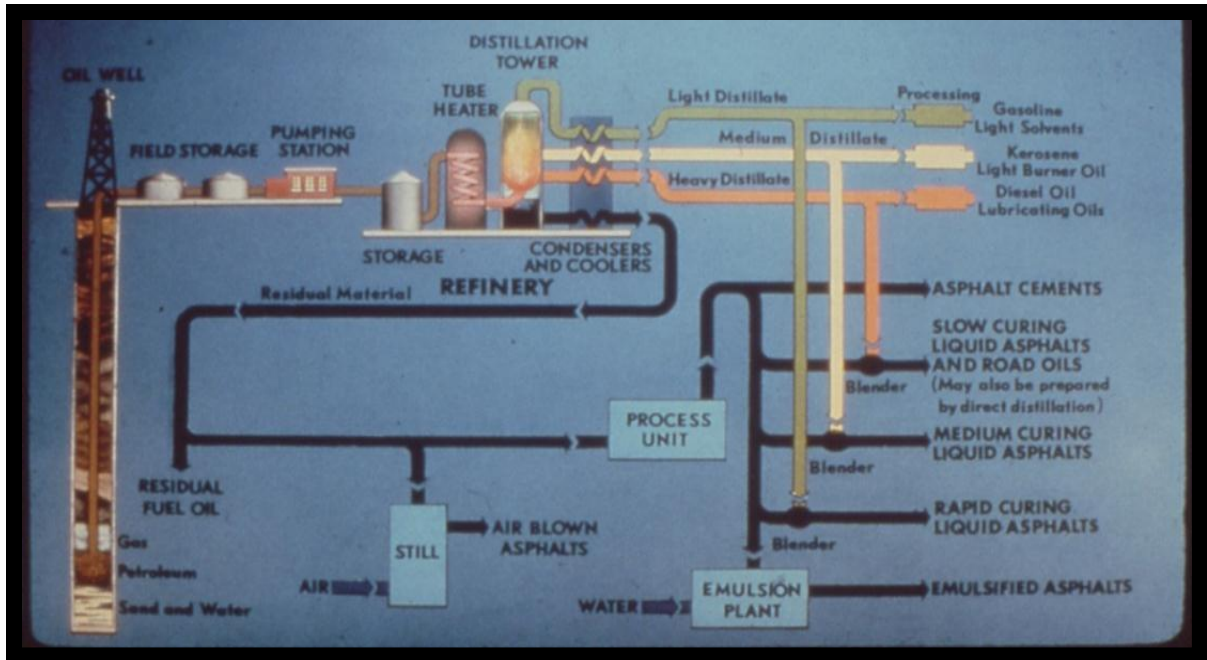


Figure 14: Schematic of asphalt production in a petroleum refinery  
 Courtesy: Western Emulsion, Inc.

### 1.3.3 Asphalt Aging

Asphalt aging is related to the occurrence of hardening or embrittlement. Asphalts harden in the paving mixture during construction and in the pavement itself. The hardening is caused mainly by oxidation. Oxidation in asphalt binders is a process that arises most readily at higher temperatures (such as construction temperature) and in thin binder films (such as the film coating aggregate particles). So, mixing is the stage at which the most severe oxidation and hardening usually occur (Chen et al. 2000). The hardening leads to the growth of several distress types, such as breakdown and rupture from both fatigue and thermal cracking distresses that causes pavement failures (Chen et al. 2000). The hardening of a binder continues in the pavement after construction.

### 1.3.4 Polyphosphoric Acid (PPA)

According to Baumgardner (2009), PPA is an inorganic polymer. It is obtained by condensation of monophosphoric acid or by hydration of  $P_2O_5$ . It has no free water, highly soluble in organics, a non-oxidant compound, and a viscous liquid ( $25^\circ C$ ) from 105%wt to 115%wt. Figure 15 shows the PPA multifarious structure; many chain lengths exist are balanced subject to concentration. The formula of PPA is shown in Figure 16. The general opinion is that PPA chemically ages or accelerates oxidative aging of asphalt. PPA acid actually has anti-oxidative characteristics, according to his research. In his conclusion, he has stated that the asphalt and crude source play an important factor in effect of asphalt modification with PPA, and also PPA is a valuable modifier to binder suppliers necessary to provide performance desired binders.

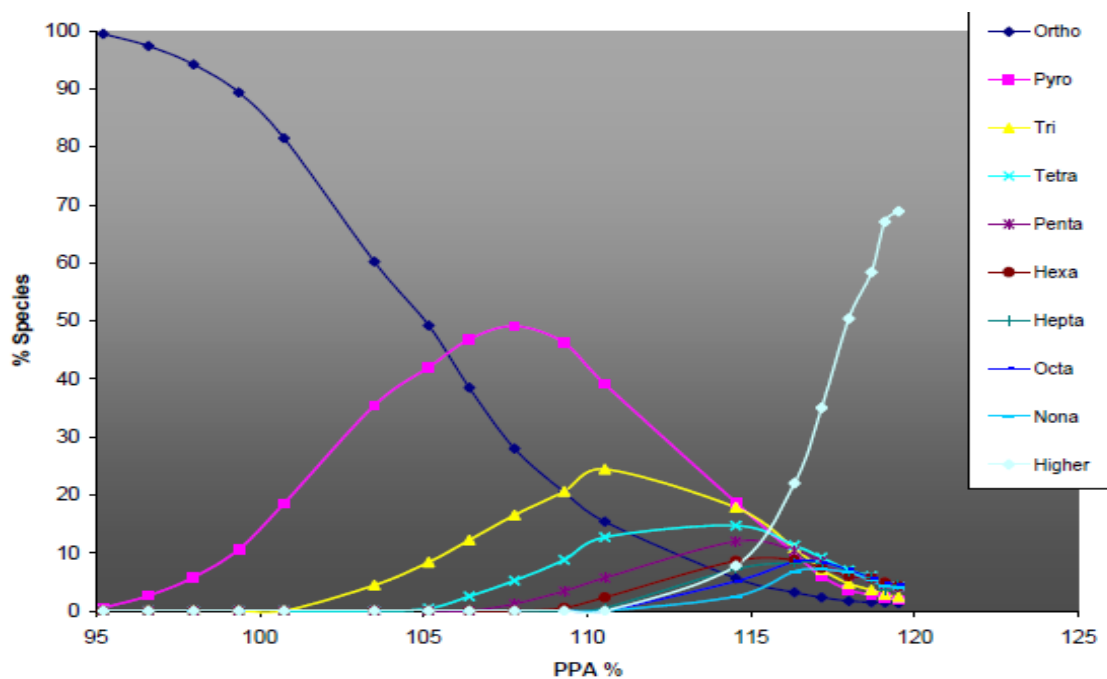


Figure 15: PPA multifarious structure

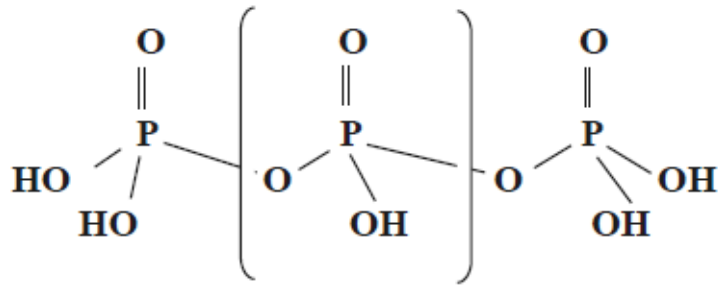


Figure 16: PPA (H<sub>3</sub>PO<sub>4</sub>) chain

### 1.3.5 Asphalt Grading System

The performance graded (PG) system is a technique used to measure asphalt binder performance. It was developed during the strategic highway research program (SHRP) in the early 1990's. The Superpave performance grading (PG) specification classifies asphalt binders into performance grades that change at 6°C intervals according to the service climate (Clayton et al. 2009). PG asphalt binders are selected to meet expected high temperature and low temperature extremes with a certain level of reliability. This increases the resistance to permanent deformation or rutting at high temperatures and increases the resistance to transverse thermal cracking at low temperatures (Clayton et al. 2009). Take for example PG 64-22, a performance grade binder used for this research. The first number (64) signifies that the binder meets high temperature physical properties up to 64°C. In contrast, the last number (-22) signifies the binder meets low temperature physical properties down to -22°C (Clayton et al. 2009). Figure 17 shows the meaning of PG 64-22 asphalt binder.

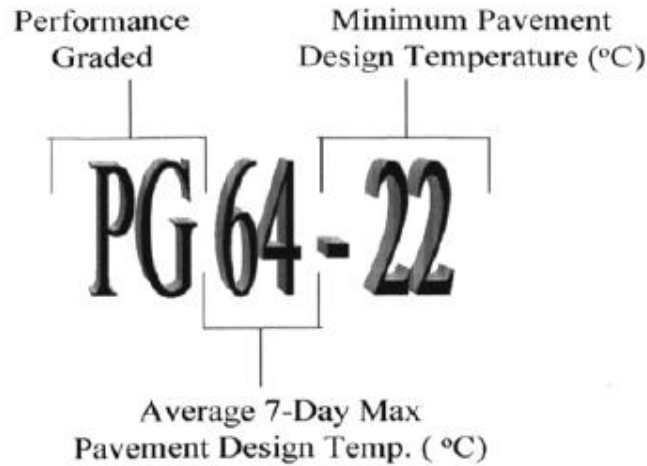


Figure 17: PG 64-22 asphalt binder

#### 1.4 Purpose of Research

The primary focus of this research is to evaluate the aging characteristics of selected modified asphalt. The characteristics of PPA added aged and unaged asphalt binders using Fourier transform infrared (FTIR) spectroscopy technique were studied. PPA modified and unmodified samples are to be tested using dynamic shear rheometer (DSR) test which characterizes both elastic modulus and flow viscosity of the asphalt binders. Finally, as a new tool, epifluorescence microscopy is beginning to gain popularity in characterization and identification of interaction between PPA and base asphalt. Epifluorescence microscopy as a new tool is used for this research as well.

#### 1.5 Research Questions

This research investigated a PG 64-22 asphalt binder supplied by a source used by TxDOT, so results obtained will provide useful information to Engineers and practitioners of TxDOT. Following questions were motive for this work:

1. What effect does addition of PPA to PG 64-22 have on enhancing viscoelastic behavior and aging resistance of the asphalt binder?
2. How does PPA react with polymer content of SBS containing asphalts? What is the interaction of PPA with asphalt?
3. What are the effects of PPA on aging characteristics of asphalt?

To answer these questions, the binders were examined using the following techniques:

- FTIR
- DSR
- Epifluorescence microscopy

## CHAPTER 2

### LITERATURE REVIEW

PPA has been used as a modifier in asphalt binders since the early 1970's to improve the performance in terms of high temperature rheological properties without adversely affecting low temperature rheological properties (De Filippis et al. 1995). A study was done by Daranga, Clopotel, Mofolasayo, and Bahia (2009) on PPA modified and unmodified binders. The asphalt binders were modified using 105% polyphosphoric acid and the amount added to the binders was 1.00 wt %. The asphalt samples were tested for  $G^*$  and  $\text{Sin } \delta$  by using dynamic shear rheometer (DSR) at a temperature of 64°C, where:

$$G^* = \tau_{max} / \gamma_{max}$$

$\delta = \text{time lag in the applied shear stress vs time plot.}$

$\tau = \text{shear stress of the asphalt.}$

$\gamma = \text{shear strain of the asphalt.}$

The results of the modified and unmodified binder showed the following:

- An increase in stiffness in the PPA modified binders compared to unmodified binders but it also depends on the type of binder used.
- PPA actually does not promote oxidation and in some binders, it actually reduces oxidation process.

According to pavement interactive (2010), asphalt binders are visco-elastic. Viscous means that it is not able to return to its original shape after a load is applied and

removed whereas elastic is when it is able to return to its original shape after a load is applied and removed. For preventing rutting and fatigue cracking,  $G^*$  and  $\delta$  are used. Asphalt binders should be stiff as well as elastic to prevent rutting. Thus, binders should have higher  $G^*/\sin \delta$ . Higher the  $G^*$ , the material is stiffer, and lower the  $\sin \delta$ , the elastic portions of  $G^*$  are more elastic. In the case of fatigue cracking, the binder should not be too stiff and must be elastic. Thus,  $G^*/\sin \delta$  should be least.

Another study was done by Huang, Turner, Miknis, Thomas (2008) where 1.5 wt % of PPA (105%) was used to investigate its effect on aging characteristics of asphalt binders. DSR and FTIR were used to measure the physical and chemical properties of aged and unaged unmodified and modified asphalt binders. Based on their study, PPA modified asphalts have the following benefits:

- By increasing the initial stiffness, it increases early resistance of the pavement to rutting.
- Improves the low-temperatures flow properties and extends the useful life of the pavement.
- Reduces both fatigue cracking and low temperature cracking.

D'Angelo (2009) has worked on the effect of PPA on high temperature binder grade, Venezuelan and Saudi Light and has used 0.5% wt PPA. PPA with polymer (SBS) modification was also done. According to his studies, 0.5% PPA increased the grade temperature of the Venezuelan to 7°C, and Saudi Light 2°C to 3°C. DSR and multiple stress creep recovery (MSCR) test was done. The test was performed at an unknown controlled shear stress using a haversine load for 1 second followed by a resting time of 9



seconds. The asphalt binder reaches a peak strain for the period of each cycle and then recovers before applying the shear stress again. Based on D'Angelo's research, the effect of PPA proved the following:

- Improved both the high temperature grade and the polymer networking in the binders.
- $G^*/\sin \delta$  indicates a larger improvement than multiple stress creep recovery (MSCR) non-recoverable compliance ( $J_{nr}$ ).  $J_{nr} = \gamma_u / \tau$  where  $\gamma_u$  is average unrecovered strain and  $\tau$  is the applied stress during creep in kPa.
- MSCR test indicates improved cross-linking.

In conclusion, his research proved that PPA does increase the stiffness of asphalt binders with the following conditions:

- The extent of the stiffening effect is dependent on asphalt binder.
- For high asphaltene Venezuelan, 0.5% PPA will increase the stiffness one full grade.
- Improves cross-linking and elastic response of SBS polymer modified asphalt binders.

Bennert (2009) has done research on polyphosphoric acid (PPA) modified asphalt binders in terms of typical mode of failure – permanent deformation, moisture sensitivity and fatigue. He has done dynamic modulus testing on PPA modified asphalt samples. The dynamic modulus testing is used to evaluate the mixture stiffness at different temperatures and loading speeds. The temperatures used for his research are 4.4, 20, and 45°C. The loading speeds are 25, 10, 5, 1, 0.5, 0.1, and 0.01 Hz. According to the

dynamic modulus testing, it showed that both modified asphalts (SBS and SBS+0.5% PPA) provided very similar modulus values after undergoing long-term oven aging. The SBS+PPA modified asphalt achieved slightly higher modulus values at higher test temperatures at the short-term oven aged condition. When evaluating the ratio between short and long term oven aged modulus, the SBS+PPA asphalt achieved slightly lower ratios than the SBS modified asphalt by itself. This may be reason of SBS modified asphalt experiencing a greater extent of age hardening when compared to the SBS+PPA modified asphalt. Fatigue evaluation was measured using a flexural beam fatigue device, AASHTO T-321 (2008) at a loading speed of 10 Hz and 20°C temperature. The test basically shows the ability of an asphalt binder sample to withstand repeated bending which causes fatigue failure also known as crack initiation. The samples were run at different tensile strains to simulate different applied loads. Based on the fatigue evaluation of Bennert's study, SBS, and SBS+PPA modified asphalt binder provided fatigue and durability resistance. His conclusions were:

- Flexural beam fatigue test results on short-term and long-term oven aged samples were at a 95% confidence level.
- Tensile strength ratio (TSR) tests showed that the SBS+PPA modified asphalt achieved a slightly higher TSR value than the SBS modified samples.

Another study by Buncher (2009) indicates that PPA can improve physical properties of asphalt when used correctly and in suitable amount. Inappropriate use of PPA can result in issues and problems. He has concluded that:

- PPA can be an effective and cost-effective tool for chemical modification, used alone or in conjunction with a polymer.
- PPA can improve high-temp PG grade, and with some asphalt sources may slightly improve low-temp PG grade.
- PPA can enhance moisture resistance.
- PPA does not work equally well in all types of asphalts and it's only asphalt chemistry dependent.

Another research was done by Le Guern, Chailleux, Farcas, Dreessen, Mabilie (2010) that focused on physico-chemical study of five different types of asphalts, both before and after aging. The aging effect was studied not only on the chemical species but also on chemical organization. Simulated aging was done by spending 25 hours in a pressure aging vessel (PAV) test. Based on the study, PPA modification increases asphaltene content and a more dispersed asphaltene structure is established than that found in pure asphalt. FTIR was used to monitor the changes in aging based on the resulting spectra's. The characteristic band of carbonyl functions C=O (approximately at around  $1700\text{ cm}^{-1}$ ) was the main focus. Monitoring the C=O band makes it possible to observe the changes in oxidation band of the binder. During aging, a change in asphalt chemistry is actually taking place; this change is due to the formation of polar groups with oxygen like ketones, acids or anhydrides. Another remarkable method used for this study is the calculation of structural indices in order to avoid the effect of the quantities being analyzed such as film thickness. The carbonyl contents were determined using CO indices as follows:

$$I_{\text{CO=}} = \frac{\text{Area of the carbonyl band centered around } 1700 \text{ cm}^{-1}}{\text{Area of the CH}_2 \text{ band centered around } 1455 \text{ cm}^{-1} + \text{Area of the CH}_3 \text{ band centered around } 1376 \text{ cm}^{-1}}$$

The research concluded that the evolution of agglomerates (spatial collection of particles that are chemically not bonded) is linearly correlated with the evolution of carbonyl band during aging. The carbonyl band actually helps to track the polarity increase in asphalt. An increase in asphalt polarity also leads to greater molecular association.

Masson and Collins (2009) did a FTIR study of the reaction of polyphosphoric acid and model asphalt sulfur compounds. According to them, sulfur is the most abundant heteroatom in asphalt, found mostly as aliphatic and aromatic sulfides. Sulfides might be the question of a nucleophilic replacement that would help to explain the decrease in asphalt molecular weight when treated with PPA. PPA is used to improve asphalt properties. When the reaction of models with a sulfur functional group was investigated, the findings showed that sulfide groups (aliphatic or aromatic), kept on inert when heated with PPA at 150°C for 1 hour. These findings nullified the assumption that nucleophilic displacement of sulfides lead to a reduction in molecular weight of asphalt. In comparison, the sulfoxide group was found to be very reactive. These findings suggest that oxidized and unoxidized asphalt would not be equally reactive toward PPA.

According to Masson, Collins, Woods, Bundalo, and Margeson (2010) PPA is used to modify asphalt in efforts to increase pavement upper service temperatures and to reduce rutting. It may also improve lower temperature properties. In their study, asphalt binders with known organic functional group contents were modified with PPA and characterized by physico-chemical techniques. From the changes PPA made on

molecular mass, asphalt microstructure, and glass transition temperatures ( $T_g$ ), a vital understanding of the mechanisms of PPA modification was found. PPA reacts with organic functional groups that contain heteroatom, specifically, oxygen, nitrogen, and sulfur. Oxidation leads to an increase in molecular mass and bigger asphaltenes content. In comparison, PPA reduces both molecular mass and true asphaltenes content. Asphaltenes are high molecular weight species.

A study was done by Khattak and Baladi (1998) on the mechanical and engineering properties of polymer (SBS) modified asphalt that showed a significant increase in indirect tensile strength and fracture toughness of asphalt mixtures at 25°C and 60°C. This indicates increased resistance to fatigue cracking and rutting. The tensile strength increases the fatigue life of the binder.

In a study for the Ohio Department of Transportation, Sargand and Kim (2001) compared the fatigue and rutting resistance of three PG 70–22 asphalt binders, one unmodified, one SBS modified, and one SBR modified. According to the study, it was found that the modified binders were more resistant to both fatigue and rutting than the neat binder (PG 70-22), even though all three had the same performance grade.

Feng and Jianying (2010) have done a study on high performance SBR modified asphalt with the addition of polyphosphoric acid (PPA), styrene-butadiene rubber (SBR, type of polymer), and sulfur. In their study, the effects of PPA, SBR, and sulfur on the physical properties (softening point, penetration, toughness, and ductility), the dynamic rheological properties (complex shear modulus,  $G^*$  and phase angle,  $\delta$ ), and the morphologies of asphalts were studied. Aging was done using the RTFO test on polymer

modified base asphalt (AH-90). FTIR spectroscopy was used to study the functional characteristics of different bands, DSR for dynamic rheological properties, ASTM D36, D5, D5801-95 and Chinese specification GB/T 4508 for physical properties, and optical microscopy for morphology observation. Based on their research, the addition of PPA can improve the high-temperature physical and rheological properties of asphalt with a critical effect on the low-temperature ductility. In contrast, SBR addition to pure PPA modified asphalt can improve the low-temperature ductility intensely whereas addition of sulfur to the PPA and SBR modified asphalt improved the high-temperature rheological properties. PPA, SBR, and sulfur modified asphalts did not show much difference in terms of rheological behavior. They have concluded that the appropriate amount of PPA, SBR, and sulfur in asphalt can improve the properties of SBR compound modified asphalt to a higher extent.

Following is a summary of different research groups who worked on PPA addition to base binders. The summary table (Table 1) presents findings of different research groups who studied various asphalt binders and effects of PPA on performance and oxidation resistance of the binders studied. As can be seen from Table 1, all groups found PPA to enhance performance of the asphalt both in laboratory testing and field evaluations, however, effects of PPA on aging show mixed results. This aspect was studied in detail in this investigation. Each research group cited in Table 1 presented their findings at the PPA Workshop Minneapolis April 7-8 2009 sponsored by Federal Highway Administration.

Table 1: Research groups who worked on PPA addition to base binders.  
The entire research group in Table 1 is reprinted from the following web page:  
<https://engineering.purdue.edu/NCSC/PPA%20Workshop/2009/index.html>

Researcher/Affiliation	PPA Concentration	Tests done (DSR/ER/Hamburg)	PG-grade evaluated	PPA prevents Aging (Yes/No)	PPA improves PG grade?	Field Testing done (Yes/No)
Arnold, Turner-Fairbank Highway Research Center (TFHRC)	115% PPA	DSR, Hamburg, X-Ray Fluorescence	76, 76, 82	No	Yes	No
Abadie, Louisiana Department of Transportation	N/A	RTFO, CR MSCR test	PG 76-22, PG 64-22	N/A	N/A	Yes
Baumgardner, Paragon Technical Services, Inc	PPA 105%, 115% (0.2, 0.4, 0.6)	DSR, RTFO, PAV, BBR	PG 64-22, PG 58-28, PG 52-34	Yes	Yes	No
Bennert, Rutgers University Center for Advanced Infrastructure and Transportation (CAIT)	0.5% PPA	Dynamic Modulus, AASHTO TP62 (STOA and LTOA), Flexible Beam Fatigue, AASHTO T321 (STOA and LTOA), Repeat Load/Flow Number (STOA), Susceptibility to Moisture Damage, AASHTO T283, Tensile Strength Ratio (TSR)	PG 64-22, 76-22	N/A	Yes	Yes
Buncher, Asphalt Institute	N/A	N/A	N/A	Yes	Yes	No
Clyne, Minnesota Department of Transportation	N/A	Hamburg, DSR, PAV, RTFO, MSCR, Longitudinal Strain, Transverse Strain, Dynamic Pressure	PG 58-34	N/A	N/A	Yes
Dangelo, Federal Highway Administration	0.50%	MSCR Test, DSR, RTFO, PAV, BBR	PG 64-22, PG 58-28	Yes	Yes	No
McGennis, Holly Asphalt Company	1% PPA	Tensile Strength Ratio (TSR)	PG 76-16, PG 70-10	N/A	N/A	Yes
Reinke Analytical, Mathy Technology & Engineering Services, Inc	105% PPA, 0%, 0.2%, 0.5%, 0.75%, 1.0%, 1.2%, 1.5%, 2.0%, 2.5%, 3.0% , 0.8%	Energy Dispersive X-Ray, Fluorescence (EDXRF), DSR	PG 64-22, PG 76-22, PG 70-22, PG 64-28, PG 58-34	N/A	N/A	Yes

Reinke Performance, Mathy Technology & Engineering Services, Inc	0.75% PPA, 0.3% PPA, 1.2% PPA, 0.6% PPA, 1% PPA	Hamburg, Tensile Strength Ratio (TSR), ICL, DSR, RTFO,	PG 58-28, PG 64-28, PG 64-34, PG 70-28 , PG 76-22, PG 67-22, PG 82, PG 64-22, PG 70-22. PG 72	N/A	N/A	No
Kai Tam,Ontario Ministry of Transportation	1% PPA, 0.5 PPA	N/A	PG 70-28, PG 70-34, and PG 64- 34	N/A	N/A	No
Vanfrank, UTAH	0.85% PPA, 0.56% PPA	DSR, Hamburg, Linear Kneading Compactor(LKC)	PG 64-34	N/A	N/A	Yes
Watson, National Center for Asphalt Technology (NCAT)	0.2, 0.4, 0.6% PPA	DSR, PAV, RTFO,	PG 76-22, PG70-22, PG67-22	N/A	N/A	Yes

\*Any item not studied is marked N/A



## CHAPTER 3

### EXPERIMENTAL PROCEDURES

Asphalt binder PG 64-22 containing 1.0, 2.0, and 3.0 wt % PPA (105%) concentration was used. The asphalt samples with PPA concentration were prepared with the base binder (PG 64-22) and 1-3% PPA mixed in a mixer with high shearing action. During this process, some of the samples could be subjected to oxidation. The purpose of this research is to investigate the effect of PPA modified characteristics of asphalt binders in terms of aging, stiffness, and interaction between PPA and base asphalt. The first analytical technique that is used is Fourier transform infrared (FTIR) spectroscopy. FTIR is being used for PPA modified and unmodified aged asphalts. Oxidation of asphalt samples were quantified by measurement of carbonyl band which is approximately at  $1650\text{ cm}^{-1}$  to  $1800\text{ cm}^{-1}$  (Peterson et al. 1993) in the spectra of FTIR. Several authors have shown that carbonyl formation is a major product of oxidation (Peterson et al. 1993). The  $\text{CH}_3$  asymmetric stretching vibration at about  $2975\text{-}2950\text{ cm}^{-1}$  and  $\text{CH}_2$  absorption at about  $2930\text{ cm}^{-1}$  are to be measured in terms of height to find out if it correlates to the amount of PPA added.

The second technique that is used is dynamic shear rheometer (DSR). DSR is used to characterize the viscous and elastic behavior of asphalt binders at given temperature. At high temperature and long loading time, asphalt binders act like high viscosity flowing fluids. At low temperatures and short loading time, they act like elastic solids. This kind of viscoelastic behavior is characterized by DSR testing. The DSR gives

a complete picture of the behavior of asphalt binders at pavement service temperature by measuring both  $G^*$  and  $\text{Sin } \delta$ .

Finally, epifluorescence microscopy is used in characterization of interaction between PPA and base asphalt. The three different parameters which are aging, stiffness, and interaction between PPA and base asphalt are explained in the next section.

### 3.1 Aging

The original materials were aged using a regular oven and RTFO test. The RTFO aged samples were analyzed using FTIR Spectroscopy, DSR, and epifluorescence microscopy test while the regular oven aged samples were tested only using epifluorescence microscopy to study effects of prolonged asphalt exposure to heat. Epifluorescence microscopy was used to study effect of heating on asphalt morphology. The next sections will discuss the tests used for this research in terms of theory, and sample preparation.

### 3.2 Regular Oven Test

#### 3.2.1 Sample Preparation

Aging experiments were conducted by placing approximately  $20\text{g} \pm 0.5$  of asphalt binders containing PPA in an oven at a temperature of  $60^\circ\text{C} \pm 0.5^\circ\text{C}$  for a period of 3 weeks. The asphalt samples were kept in a sealed plastic bottle to avoid atmospheric oxygen. The asphalt samples were characterized every week to observe the changes in epifluorescence images due to PPA interactions with both SBS containing and plain asphalt samples. Table 2 shows different types of samples studied for the interaction of

PPA and asphalt. All PPA containing samples were prepared in a proprietary process and supplied by Innophos Company.

Table 2: Analysis matrix table for PPA-asphalt interaction study

<b>SAMPLES</b>
PG 64-22
PG 64-22 + 1% PPA
PG 64-22 + 2% PPA
PG 64-22 + 3% PPA
PG 64-22 + 2%SBS + 0.1%S
PG 64-22 + 2%SBS + 0.1%S + 1%PPA
PG 64-22 + 2%SBS + 0.1%S + 2%PPA
PG 64-22 + 2%SBS + 0.1%S + 3%PPA

### 3.3 Rolling Thin Film Oven (RTFO)

#### 3.3.1 Theory

To promote short term aging, RTFO test (Figure 18) was used. RTFO test is used to simulate aging in asphalt binders illustrative of the aging that occurs during mixing or construction of pavements. The RTFO test ages asphalt binder samples by exposing them to heat and air flow continuously to promote oxidation which leads to aging. The RTFO procedure basically uses cylindrical bottles that contain the asphalt binder samples which are then placed in a rotating carriage within an oven. The carriage rotates within the oven while the 325°F (163°C) temperature ages the samples for 85 minutes. Then, the samples are tested using FTIR, DSR, and Epifluorescence microscopy tests.



Figure 18: Rolling thin film oven test  
Courtesy: Controls Testing Equipment, 2007

### 3.3.2 Sample Preparation

1. Heat up the oven for at least 2 hours with the temperature control set at  $163^{\circ}\text{C}$  ( $325^{\circ}\text{F}$ ), with the air on, and with the flow rate fixed at  $4 \text{ L/min} \pm 0.2 \text{ L/min}$ .
2. Heat a sample of asphalt binder until it is liquefied. Stir sample to ensure uniformity and eliminate air bubbles.
3. Pour  $35 \pm 0.5 \text{ g}$  of asphalt binder into a sample bottle. After that, place the bottles in the RTFO oven carousel, and rotate carousel at 15 RPM for 85 minutes. During this time, do not change the oven temperature and airflow rate.
4. After 85 minutes (aging is done), remove the bottles one at a time and take out residue from each bottle by first pouring as much material as possible. Scrap the sides of the bottle to remove any remainder. Any test should be done within 72 hours of aging.

### 3.4 Analytical Techniques to be Utilized

Degree of aging and influence of aging on physical characteristics of PPA added asphalt will be investigated using FTIR and epifluorescence microscopy and results will

be correlated to mechanical characteristics of binders using DSR. Following sections describe fundamentals of each technique along with typical output and interpretation of the results.

### 3.5 Fourier Transform Infrared Spectroscopy (FTIR)

#### 3.5.1 Theory

One of the main focuses of this research is the applicability of Fourier transform infrared spectroscopy (FTIR) in studying asphalt degradation due to aging. Quantification of the oxygen uptake during aging is a direct measure of the advancement of the aging process (Glover, 2007). As said earlier, the FTIR spectroscopy was used for quantification of carboxylic acid concentration (carbonyl) during the aging of asphalts.

FTIR spectroscopy is used as a measuring tool for collecting infrared spectra to find the phase contents of a sample. Instead of recording the amount of energy absorbed when the frequency of the infra-red light is varied (monochromator), the infra-red light is guided through an interferometer. After passing through the sample, the measured signal is the interferogram. Performing a fourier transform on this signal data results in a spectrum identical to that from conventional (dispersive) infrared spectroscopy. FTIR spectrometers are cheaper than conventional spectrometers as building an interferometer is easier than the fabrication of a monochromator. In addition, measurement of a single spectrum is faster for the FTIR technique as the information at all frequencies is collected simultaneously. This allows multiple samples to be collected and averaged together resulting in an improvement in sensitivity. Virtually all modern infrared spectrometers are FTIR instruments (Harwood, 1989). The results generated through FTIR analysis are

referred to as an infrared spectrum. The spectrum graphically illustrates the relative intensity of the energy absorbed on the y-axis versus the frequency of the energy on the x-axis. The frequency of the energy can be represented directly in microns ( $\mu\text{m}$ ) or, more popularly, as reciprocal centimeters ( $\text{cm}^{-1}$ ) referred to as wave numbers.

A beam of infrared light is produced and split into two separate beams. One beam is passed through the sample, and the other beam passed through a reference which is often the substance the sample is dissolved in. The beams are both reflected back towards a detector (Figure 19) however they first pass through a splitter which quickly alternates which of the two beams enters the detector. The two signals are then compared and a printout is obtained.

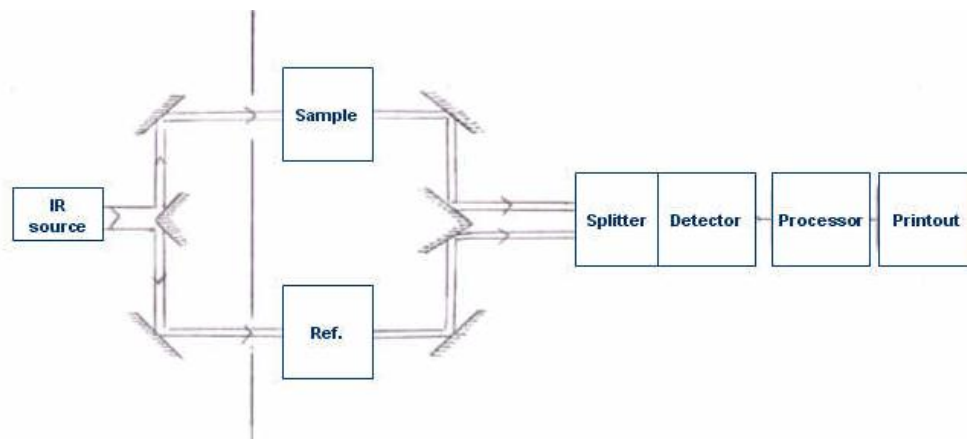


Figure 19: Schematic of FTIR apparatus

### 3.5.2 Sample Preparation

FTIR analysis was done on a Thermo Nicolet Avatar 370 DTGS from 4000 to 400  $\text{cm}^{-1}$  using 32 scans with a resolution of 4  $\text{cm}^{-1}$ . Approximately ten grams of an asphalt sample is placed on a wax sheet, and placed under a fume hood. A specially purified salt, potassium bromide (KBr) is used to make a pellet. 100 mg of KBr is pressed in a 13 mm mechanical die press to form the translucent pellet through which the beam of the

spectrometer can pass (Harwood, 1989). KBr is pressed in the die under 12,000 psi for two to three minutes to achieve the desired solid KBr pellet.

This pellet is then placed on top of the asphalt sample that was previously prepared on wax paper, to achieve a thin transparent coat of asphalt on the pellet. Light cannot pass through if the coat is too thick, so that needs special attention. Each sample is analyzed five independent times to ensure repeatability of results. The area under the carbonyl band was analyzed using the EZ OMNIC software which also gives the spectrum for the FTIR tested samples. Figure 20 shows the approach used to measure the area of the carbonyl band using the EZ OMNIC software. Not only that, the difference between a polymer and non-polymer asphalt binder will be shown. Data were saved in an Excel file and the areas were analyzed. Figure 21 is a FTIR spectrum of a PG 64-22 + 3% PPA asphalt binder.

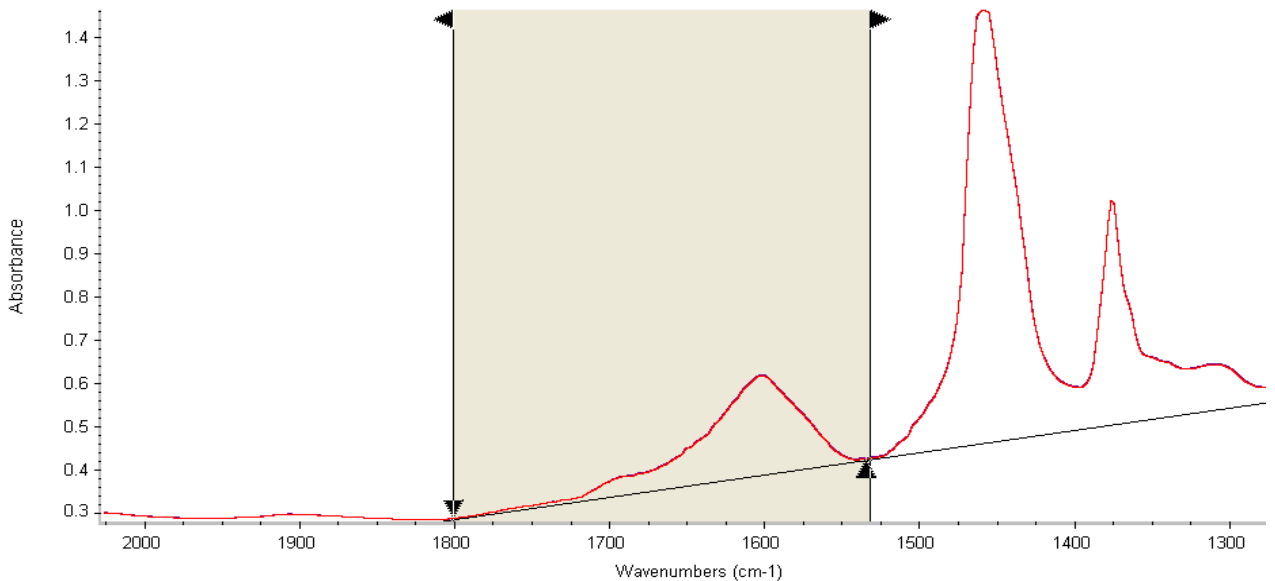


Figure 20: Measurement of the area of the carbonyl band

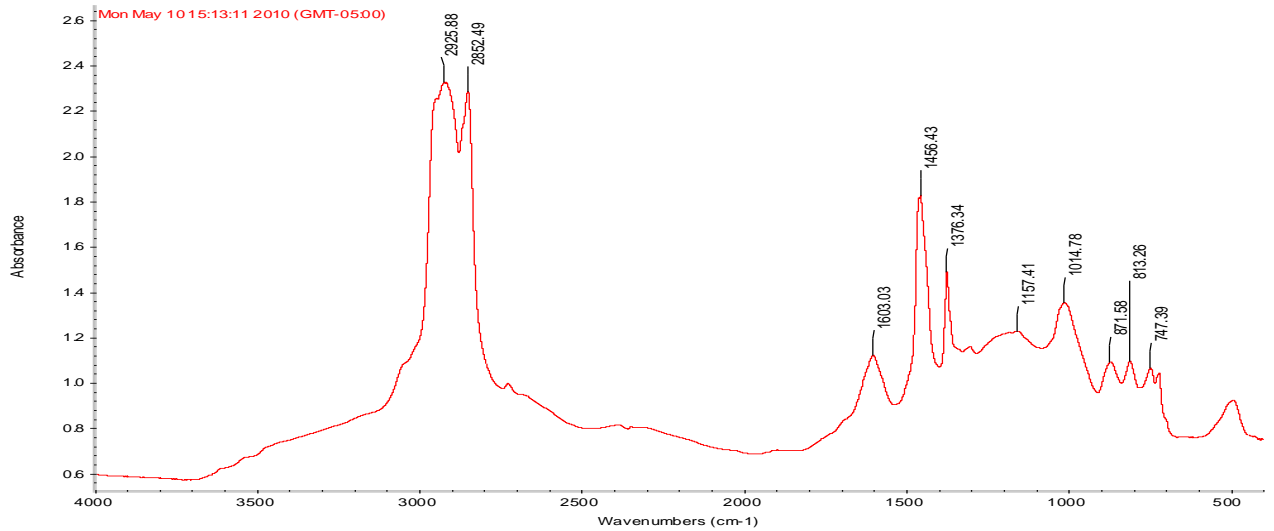


Figure 21: FTIR spectrum of a PG 64-22 + 3% PPA asphalt

### 3.6 Dynamic Shear Rheometer (DSR)

#### 3.6.1 Theory

DSR (Figure 22) was used to measure visco-elastic properties. DSR measures both viscous and elastic behavior of asphalt binders at a given temperature by determining two important rheological parameters used to predict pavement performance. The first being complex shear modulus,  $G^*$  and second being the phase angle,  $\text{Sin } \delta$ . The shear modulus relates to the total resistance of the binder to deformation while the phase angle relates to thermal cracking at low temperatures and to rutting at high temperatures. To measure these parameters, a 1mm thick by 25mm diameter specimen is compressed between two parallel plates, one that is fixed and one that oscillates. The lower plate is fixed while the upper plate oscillates back and forth across the sample at 10 rad/sec or approximately 1.59 Hz. A shear stress (Pa) is applied on the sample and the resulting strain and time lag ( $\delta$ ) determines the reaction of the binder. Testing temperatures range



from 5 to 75°C, in this case 64°C. Since the testing temperature is between 40 to 75°C, it is considered to be high temperature testing. Lower temperature testing is used for fatigue cracking characterization while high temperature testing is used to characterize rutting performance.



Figure 22: Image of dynamic shear rheometer  
Courtesy: Gecan, 2007

### 3.6.2 Sample Preparation

Samples that were prepared with the RTFO aging test was used for the DSR test. The asphalt was poured into a mold and was left to cool down at room temperature for approximately 20 minutes until it could be removed from the mold without any damage. The DSR was preheated to a temperature of 64°C prior to placing of the test sample. While waiting for the system to reach temperature equilibrium, the sample was placed on the upper plate of the rheometer as it was lowered into place at the specified height above the bottom plate. For testing at temperatures above 40°C, a sample with a height of 1mm

and a diameter of 25mm was used. For testing at temperatures below 40°C, a sample having a height of 2mm and a diameter of 8mm was used. Sample was placed in the rheometer and the plates were adjusted. The sample was trimmed with a hot spatula such that the side of the sample was perpendicular to the plate surfaces (Figure 23). The sample was submerged in water at the test temperature and the water is circulated by a circulator which heats and cools the water. Following this preparation, the sample was subjected to testing.

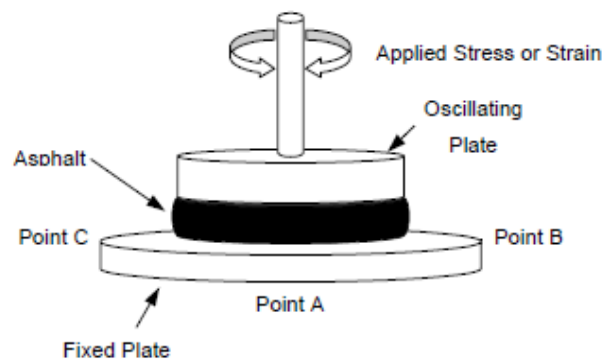


Figure 23: DSR plate setup  
Courtesy: Reubush, 1999

### 3.7 Epifluorescence Microscopy

#### 3.7.1 Theory

Epifluorescence microscopy (Figure 24) is a light tool used to study properties of organic or inorganic substances. The excitatory light is passed from below, through the lens and then onto the specimen. The fluorescence in the specimen gives rise to emitted light which is focused on the detector by the same lens that is used for the excitation. A filter between the objective and the detector filters out the excitation light from fluorescent light. Since most of the excitatory light is transmitted through the specimen,

only reflected excitatory light reaches the lens together with the emitted light. Epifluorescence microscopy creates a much higher intensity and image clarity.



Figure 24: Epifluorescence microscopy  
Courtesy: Confocal Microscope Laboratory, 2009

### 3.7.2 Sample Preparations

To make the Epifluorescence microscopy slides, the asphalt samples were heated at a temperature of  $155^{\circ}\text{C}$  -  $160^{\circ}\text{C}$  till it melts. Once the sample has melted, a slight amount of the sample was poured onto a glass slide. Then, another slide was immediately placed on top and the top slide was pressed down until the asphalt would not squeeze anymore under light pressure. This glass slides that contained the samples were tested. At least 3 – 4 images of each sample were taken using 40x settings and these images were adjusted using the ImageJ software. Table 3 shows the effective sizes for each magnification as measured on May 27th 2008 and the column highlighted in blue is the 40x used for samples testing.

Table 3: Effective sizes for each magnification

<b>Lens</b>	<b>Pixel Sizes in um</b>	<b>Micrometers per pixel</b>
5	1.3908	0.719
8	0.8978	1.114
20	0.3456	2.894
32	0.2242	4.46
40	0.1727	5.79
63	0.1116	8.961
64	0.1119	8.937
100	0.0692	14.5
101	0.0725	13.8
160	0.0448	22.3

### 3.8 Design of Experiments (DOE)

The DOE was conducted using three different asphalt binders:

1. Neat binder
2. SBS only modified
3. SBS + PPA modified

Table 4 shows the asphalt samples used for this research.

Table 4: Asphalt samples used for this research

<b>Sample Type</b>	<b>Aged/Unaged</b>	<b>Analytical Type</b>
PG 64-22	✓	DSR + FTIR + Epifluorescence
PG 64-22 + 1% PPA	✓	DSR + FTIR + Epifluorescence
PG 64-22 + 2% PPA	✓	DSR + FTIR + Epifluorescence
PG 64-22 + 3% PPA	✓	DSR + FTIR + Epifluorescence
PG 64-22 + 2%SBS + 0.1%S	✓	DSR + FTIR + Epifluorescence
PG 64-22 + 2%SBS + 0.1%S + 1%PPA	✓	DSR + FTIR + Epifluorescence
PG 64-22 + 2%SBS + 0.1%S + 2%PPA	✓	DSR + FTIR + Epifluorescence
PG 64-22 + 2%SBS + 0.1%S + 3%PPA	✓	DSR + FTIR + Epifluorescence

### 3.8.1 Aging Protocols

Samples were kept for 3 weeks at a constant temperature of  $60^{\circ}\text{C} \pm 0.5^{\circ}\text{C}$  at atmospheric temperature using a regular oven. Table 5 shows different types of asphalt samples that were kept for three weeks.

Table 5: Asphalt samples kept for 3 weeks

<b>Sample Type</b>	<b>Time (Weeks)</b>
PG 64-22	1, 2, 3
PG 64-22 + 1% PPA	1, 2, 3
PG 64-22 + 2% PPA	1, 2, 3
PG 64-22 + 3% PPA	1, 2, 3
PG 64-22 + 2%SBS + 0.1%S	1, 2, 3
PG 64-22 + 2%SBS + 0.1%S + 1%PPA	1, 2, 3
PG 64-22 + 2%SBS + 0.1%S + 2%PPA	1, 2, 3
PG 64-22 + 2%SBS + 0.1%S + 3%PPA	1, 2, 3

## CHAPTER 4

### RESULTS AND DISCUSSIONS

#### 4.1 Dynamic Shear Rheometer Results

DSR is a commonly used testing method that measures rutting and fatigue cracking resistance characteristics of asphalt binders. This test measures both viscous and elastic behavior of asphalt binders at a given temperature. Figure 25 shows plots of shear stress ( $\tau$ ) vs time (a) and shear strain ( $\gamma$ ) vs time (b) for hypothetical asphalt binder. Table 6 shows DSR results of samples aged through a rolling thin film oven test. Samples containing polyphosphoric acid with and without 2% polymer were analyzed and data was compared with that of neat binder (PG 64-22). As indicated earlier, complex shear modulus ( $G^*$ ) which is considered to be asphalt samples total resistance to deformation when repeatedly sheared was measured and results are tabulated in Table 6. Values of lag between the applied shear stress and the resulting shear strain is also measured and tabulated in Table 6. Purely elastic materials show  $\delta=0^\circ$  degrees and purely viscous materials show  $\delta=90^\circ$ . Generally the larger the phase angle ( $\delta$ ), the more viscous the material is.

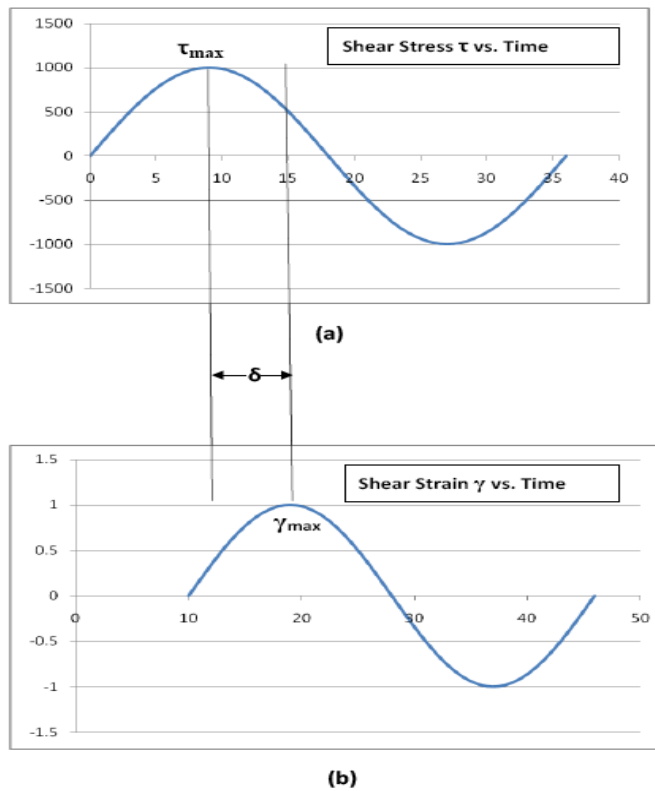


Figure 25: Plots of shear stress ( $\tau$ ) vs time (a) and shear strain ( $\gamma$ ) vs time (b) for hypothetical asphalt binder

Table 6: DSR results of RTFO aged asphalt samples

SAMPLES	$G^*/\sin \delta$ , KPa	Complex Modulus, $G^*$ KPa	Phase Angle, $\delta^*$	Strain, %
PG 64-22	3.15	3.15	86.20	6.99
PG 64-22 + 1% PPA	4.91	4.80	78.20	4.59
PG 64-22 + 2% PPA	10.50	9.88	70.50	2.23
PG 64-22 + 3% PPA	14.20	12.70	63.20	1.73
PG 64-22 + 2%SBS + 0.1%S	5.93	5.83	79.20	3.78
PG 64-22 + 2%SBS + 0.1%S + 1%PPA	19.90	15.00	49.10	1.47
PG 64-22 + 2%SBS + 0.1%S + 2%PPA	9.42	7.79	55.80	2.83
PG 64-22 + 2%SBS + 0.1%S + 3%PPA	26.20	17.40	41.70	1.27

DSR analysis was done using shear stress (Pa), temperature ( $^{\circ}\text{C}$ ), and frequency (rad/sec) as 220 Pa,  $64.01^{\circ}\text{C}$  and 10.03 rad/sec respectively. Based on data in Table 6, one can conclude that higher the PPA added, higher the  $G^*/\text{Sin } \delta$  (Figure 26). Addition of 2% SBS to the neat binder (PG 64-22), show that  $G^*/\text{Sin } \delta$  has almost doubled (Figure 27). It also seen that addition of PPA to polymer containing asphalt binder, increases the  $G^*/\text{Sin } \delta$  by more than four times (Figure 28). In all these three cases, only one common asphalt binder, PG 64-22 + 2%SBS + 0.1%S + 2%PPA that does seem to increase in terms of  $G^*/\text{Sin } \delta$  but at a smaller scale.

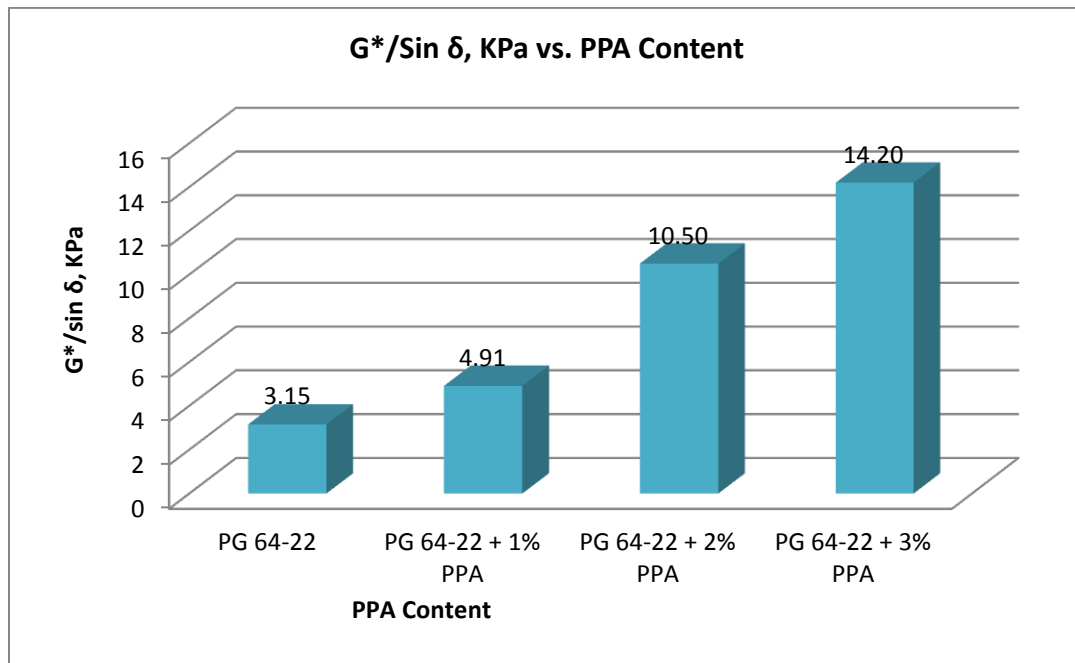


Figure 26: Comparison of  $G^*/\text{Sin } \delta$ , KPa vs. PPA containing asphalt



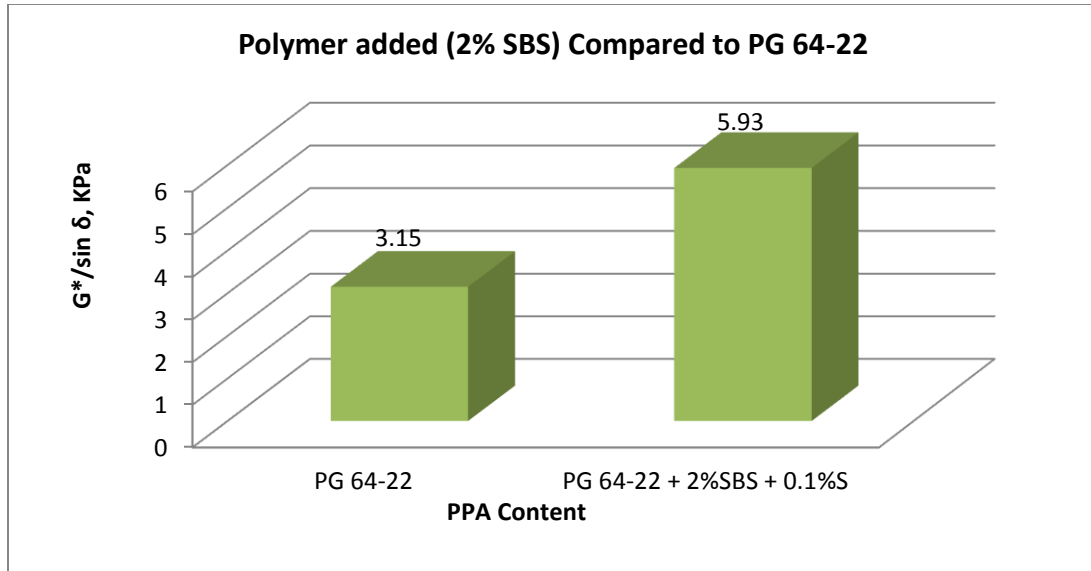


Figure 27: Comparison of  $G^*/\sin \delta$ , KPa for 2% SBS polymer added asphalt compared to neat binder PG 64-22

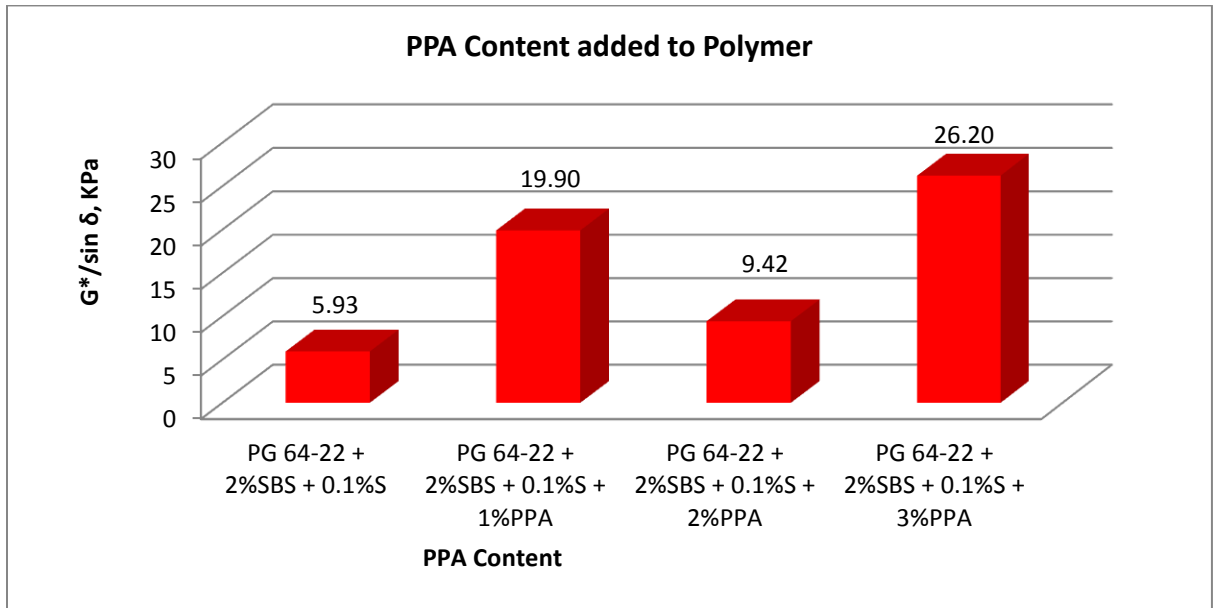


Figure 28: Comparison of  $G^*/\sin \delta$ , KPa for synergistic effects of PPA (1-3%) containing 2% SBS asphalt

Asphalts that resist rutting are stiff (offer resistance to excessive deformation) while demonstrate an acceptable degree of elasticity (ability to return to original shape)

after deformation). Such materials are expected to show high  $G^*/\sin \delta$ . Better description of  $G^*/\sin \delta$  is given in Figure 29. Considering data obtained and reported in Table 6, it appears that higher the concentration of PPA higher the  $G^*/\sin \delta$  with a linear relationship showing  $R^2= 0.86$  as seen in Figure 30. Slope of this plot indicates a factor of 5X improvement in  $G^*/\sin \delta$  values when 1-3% PPA is added to a non-polymer containing binder. When similar analysis was done for polymer containing asphalt binder PG 64-22 (without consideration of data for 2% PPA) nearly same trend showing increase in  $G^*/\sin \delta$  with PPA addition was observed (Figure 31). Results presented in Table 6 and Figure 34 indicates that combination of Polymer and PPA addition demonstrates a synergistic effect that enhances performance of PG 64-22 binder. Explanation of possible interactions between polymer, PPA and binders are considered and discussions will follow. For an unknown reason only the data for 2% PPA sample did not fit the observed trend.

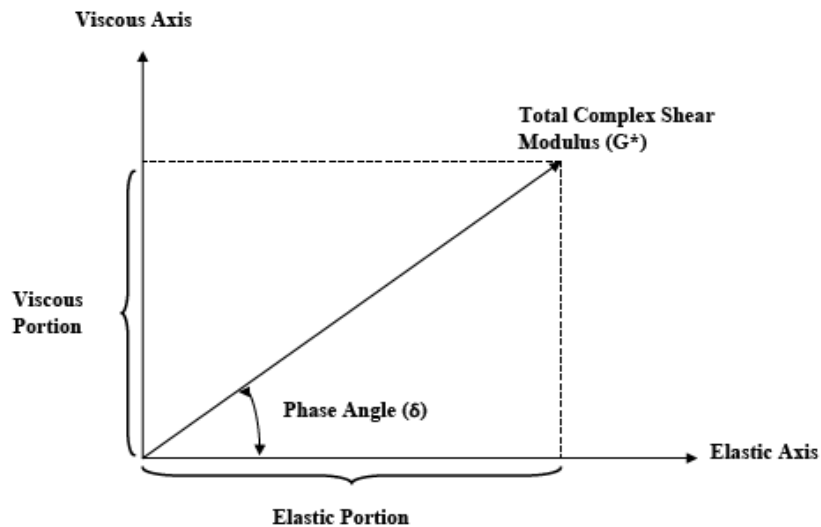


Figure 29: Plot of correlation between viscous and elastic behavior of asphalt binders.  
 Courtesy: Pavement Interactive, 2010.

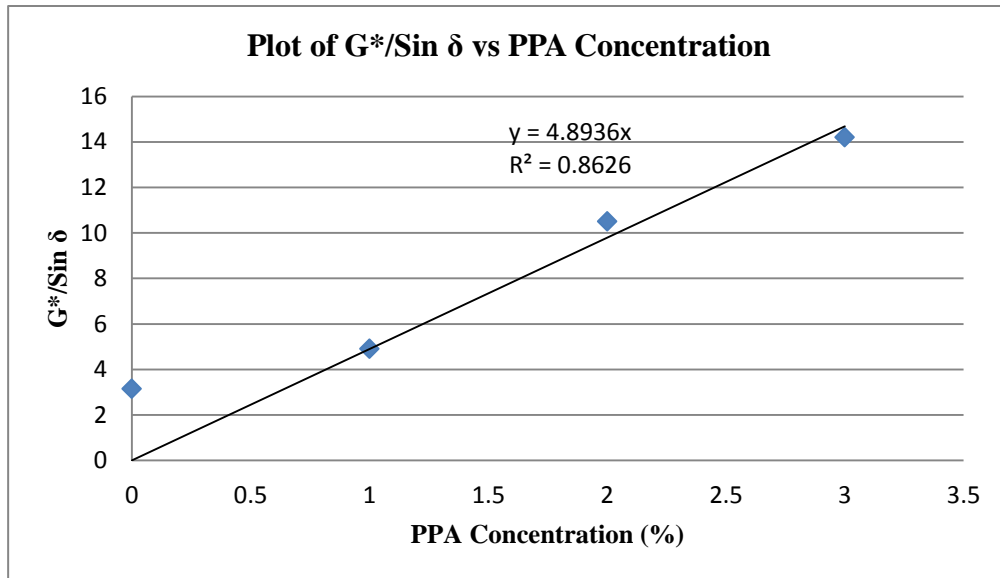


Figure 30: G\*/Sin δ for PPA containing neat binder without polymer.

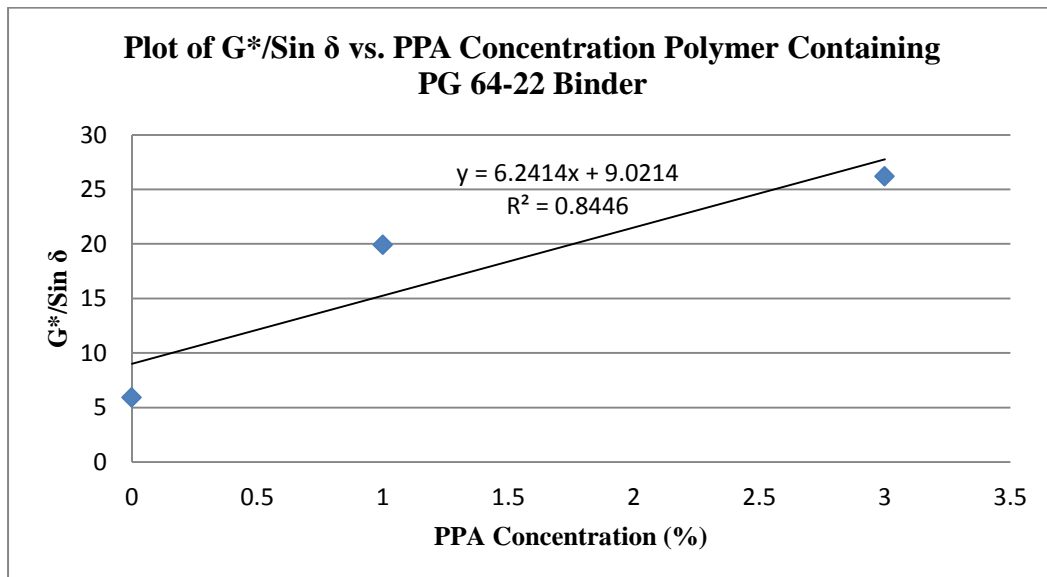


Figure 31: Plot of G\*/Sin δ vs. PPA concentration polymer containing PG 64-22 binder

Results of G\*/Sin δ presented above were compared with data obtained at Turner-Fairbank Highway Research Center (Arnold, et al. 2008) presented at the PPA workshop in Minneapolis April 2009 and a harmony was found. Their results indicated G\*/Sinδ of

about 3 KPa for a 1% PPA added binder that corresponds to 4.91 KPa obtained in this study. The binder used by Turner-Fairbank lab was a commercial PG 64-28 with 2% and 3% PPA showing  $G^*/\text{Sin}\delta$  of 7 and 17 KPa respectively. Corresponding  $G^*/\text{Sin}\delta$  values in this study are 10.5 and 14.2 KPa but DSR test was run at a temperature of 64 °C for 105% PPA added sample. They tested the commercial PG 64-28 binders at 70°C whereas tests done in this research was done at 64°C. This difference in test temperature will impact results. In summary, PPA addition to PG 64-22 is anticipated to reduce road rutting due to the fact that increase in  $G^*/\text{Sin}\delta$  lowers work dissipated per cycle ( $W_c$ ) as  $G^*/\text{Sin}\delta$  and  $W_c$  are inversely proportional (Pavement Interactive, 2010).

#### 4.2 Aging Analysis Using FTIR Spectroscopy

The FTIR analysis was performed on samples aged in rolling thin film oven. FTIR spectra of samples aged in RTFO process that was done before DSR testing were compared with their un-aged counterparts and were analyzed for quantification of degree of aging. FTIR spectra of PPA and PG 64-22 are shown in Figure 32(a) and (b) respectively to establish a baseline for identification of absorption bands. Major FTIR absorption bands of PPA include  $1012\text{ cm}^{-1}$ ,  $933\text{ cm}^{-1}$ ,  $772\text{ cm}^{-1}$ , and  $478\text{ cm}^{-1}$  (Zhang and Yu, 2010). Absorption bands related to PG 64-22 include  $2922\text{ cm}^{-1}$  ( $\nu_{\text{as}}\text{CH}_2\text{CH}_3$ ),  $2882\text{ cm}^{-1}$  ( $\nu_{\text{s}}\text{CH}_2\text{CH}_3$ ),  $1601\text{ cm}^{-1}$  ( $\nu\text{C}=\text{C}$ ),  $1455\text{ cm}^{-1}$ ,  $1376\text{ cm}^{-1}$ ,  $1031\text{ cm}^{-1}$  ( $\nu\text{SO}_2$ ),  $868\text{ cm}^{-1}$ ,  $813\text{ cm}^{-1}$  ( $\text{C}=\text{C}$ ),  $747\text{ cm}^{-1}$ , and  $722\text{ cm}^{-1}$  (Lamontagne et al. 2001).

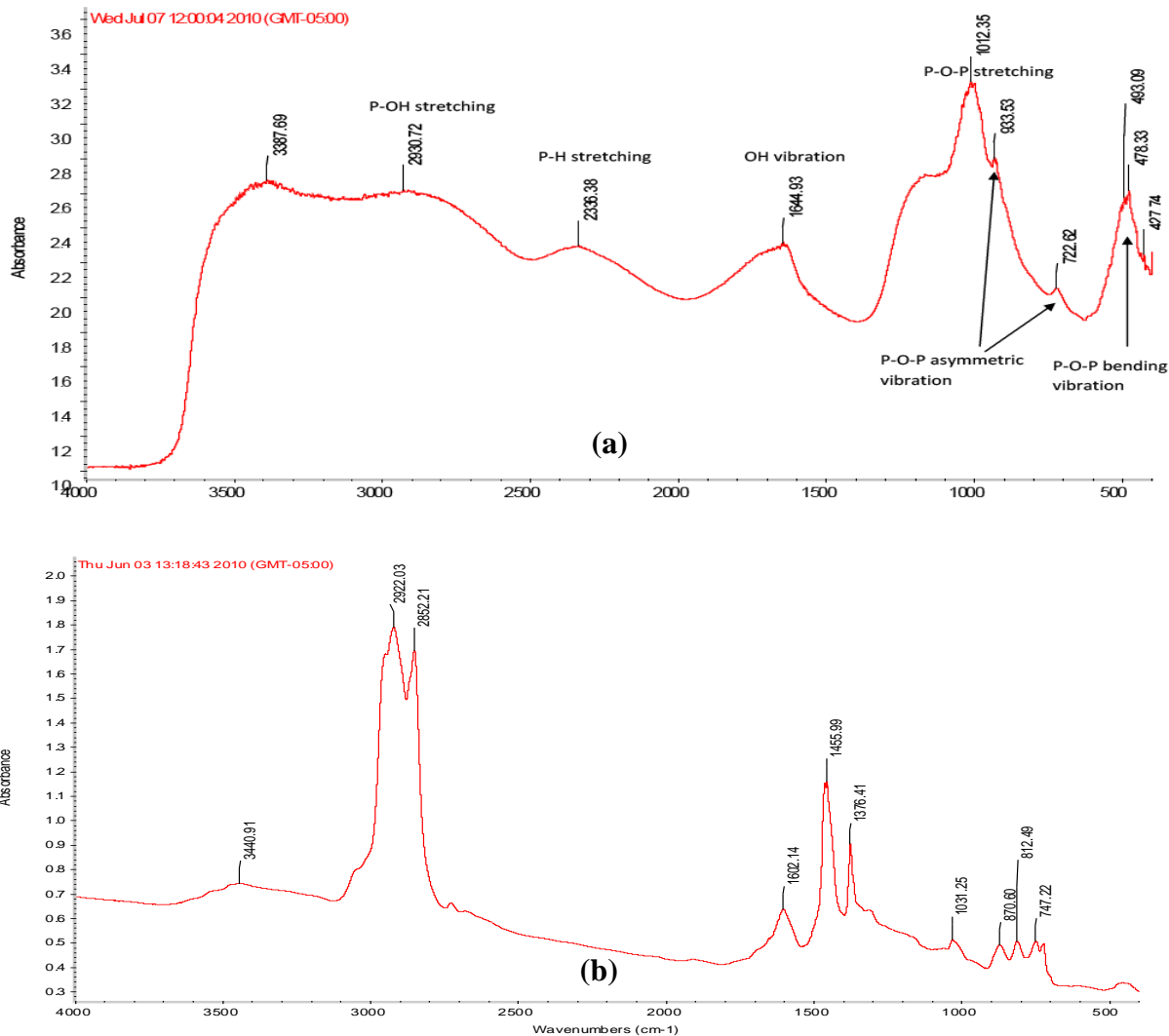


Figure 32: FTIR spectra of polyphosphoric acid (a) and PG 64-22 asphalt binder (b).

#### 4.2.1 Aliphatic Groups

Aliphatic groups are found in many compounds that the infrared spectroscopist is likely to come across. The most important vibrational modes are the C-H stretching around 3000 cm<sup>-1</sup> and the -CH deformation modes around 1460 cm<sup>-1</sup> and 1380 cm<sup>-1</sup>. The sections 4.2.2 to 4.2.5 are a courtesy of the help section from Thermo Nicolet Avatar 370 DTGS, the FTIR instrument.

#### 4.2.2 CH<sub>3</sub> and –CH<sub>2</sub> Stretching Absorptions

The CH<sub>3</sub> asymmetric stretching vibration takes place at about 2975-2950 cm<sup>-1</sup> while the CH<sub>2</sub> absorption occurs at about 2930 cm<sup>-1</sup> (Figure 33). The symmetric CH<sub>3</sub> vibration occurs at about 2885-2865 cm<sup>-1</sup> while the CH<sub>2</sub> absorption occurs at about 2870-2840 cm<sup>-1</sup>.

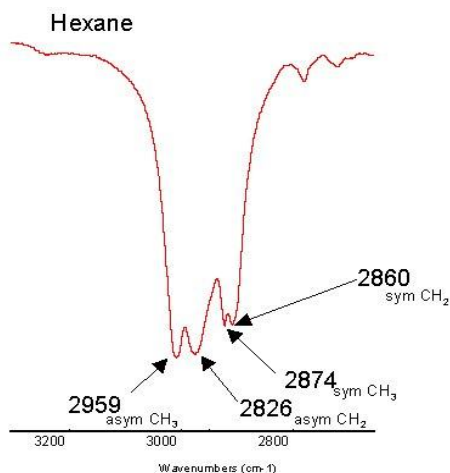


Figure 33: CH<sub>3</sub> and –CH<sub>2</sub> stretching absorptions  
Courtesy: Thermo Nicolet Avatar 370 DTGS

#### 4.2.3 CH<sub>3</sub> Deformation Absorptions

The CH<sub>3</sub> asymmetric deformation vibration occurs at about 1470-1440 cm<sup>-1</sup>. This band is coincided with the CH<sub>2</sub> scissor vibration which occurs at about 1490-1440 cm<sup>-1</sup>. The symmetric CH<sub>3</sub> vibration occurs at about 1390-1370 cm<sup>-1</sup>. The relative intensities of the asymmetric CH<sub>3</sub> and the CH<sub>2</sub> scissor bands can be used as a sign of their proportions in the molecule (Figure 34).

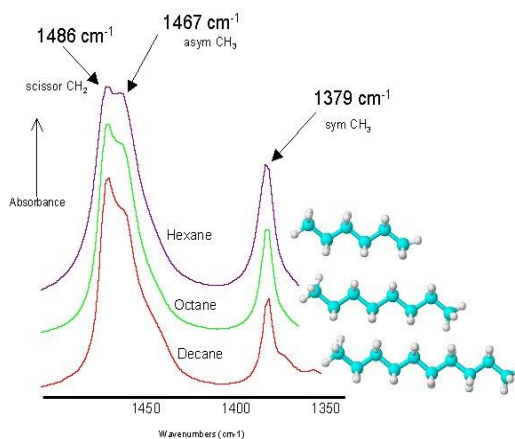


Figure 34: CH<sub>3</sub> deformation absorptions  
 Courtesy: Thermo Nicolet Avatar 370 DTGS

#### 4.2.4 CH<sub>3</sub> Deformation Absorption Band Splitting

The symmetric CH<sub>3</sub> vibration (1390-1370 cm<sup>-1</sup>) separates into two bands when there are more than one methyl group on a single carbon (Figure 35). When three methyl groups are on a single carbon (t-butyl), a band appears near 1365 cm<sup>-1</sup> and a weaker band appears close to 1390 cm<sup>-1</sup>. When two methyl groups are on a single carbon (isopropyl), bands of approximately equal intensity occur at around 1390 and 1365 cm<sup>-1</sup>.

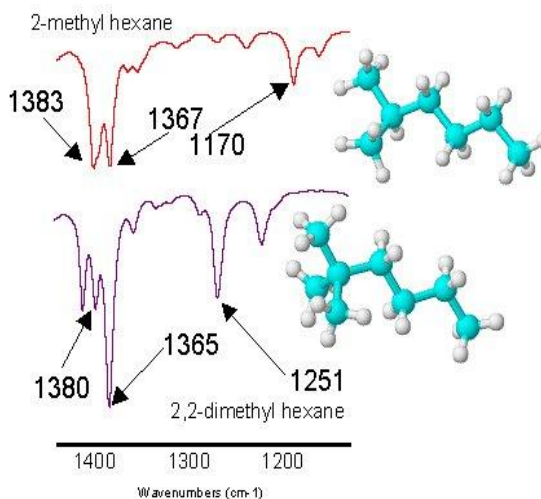


Figure 35: CH<sub>3</sub> deformation absorption band splitting  
 Courtesy: Thermo Nicolet Avatar 370 DTGS

### 4.3 Effect of RTFO Aging on CH<sub>3</sub> and CH<sub>2</sub> Proportions

Sections 4.2.1 to 4.2.4 discussed on CH<sub>3</sub> and CH<sub>2</sub>. As stated earlier, the height of the components is to be measured in terms of height (as measured for 2922 cm<sup>-1</sup> and 2852 cm<sup>-1</sup> bands) to find out if it correlates to the amount of PPA added. Table 7 shows the results obtained from the measured heights of CH<sub>3</sub> and CH<sub>2</sub> calculated based on 2922 cm<sup>-1</sup> band for CH<sub>3</sub> and 2852 cm<sup>-1</sup> for CH<sub>2</sub>.

Table 7: Results of CH<sub>3</sub> and CH<sub>2</sub>

<b>SAMPLES</b>	<b>CH<sub>3</sub></b>	<b>CH<sub>2</sub></b>	<b>CH<sub>3</sub>/CH<sub>2</sub></b>
PG 64-22	2.70	2.40	1.13
PG 64-22 + 1% PPA	1.70	1.50	1.13
PG 64-22 + 2% PPA	1.40	1.00	1.40
PG 64-22 + 3% PPA	-	-	1.00
PG 64-22 + 2%SBS + 0.1%S	2.60	2.00	1.30
PG 64-22 + 2%SBS + 0.1%S + 1%PPA	1.00	0.90	1.11
PG 64-22 + 2%SBS + 0.1%S + 2%PPA	2.80	2.50	1.12
PG 64-22 + 2%SBS + 0.1%S + 3%PPA	-	-	1.00

Based on the results from Table 7, the two asphalt binders that contain 3% PPA seem to have a value of 1.00 in terms of CH<sub>3</sub>/CH<sub>2</sub>. This is proven in Figure 36, when the 3% PPA sample is overlaid on a non PPA containing sample. The CH<sub>3</sub> and CH<sub>2</sub> components are on the equal range which gives us a CH<sub>3</sub>/CH<sub>2</sub> a value of 1.00. This again proves that with higher the PPA content, there seem to be good amount of structural changes in the binder molecular structure. As indicated in Figure 36, addition of 3% PPA to PG 64-22 broaden the absorption bands at 2922 cm<sup>-1</sup> and 2852 cm<sup>-1</sup> indicating random (mixed asymmetric and symmetric vibrations) of both CH<sub>3</sub> and CH<sub>2</sub> constituents. Same phenomenon is observed in asphalt binders with and without polymer (SBS).



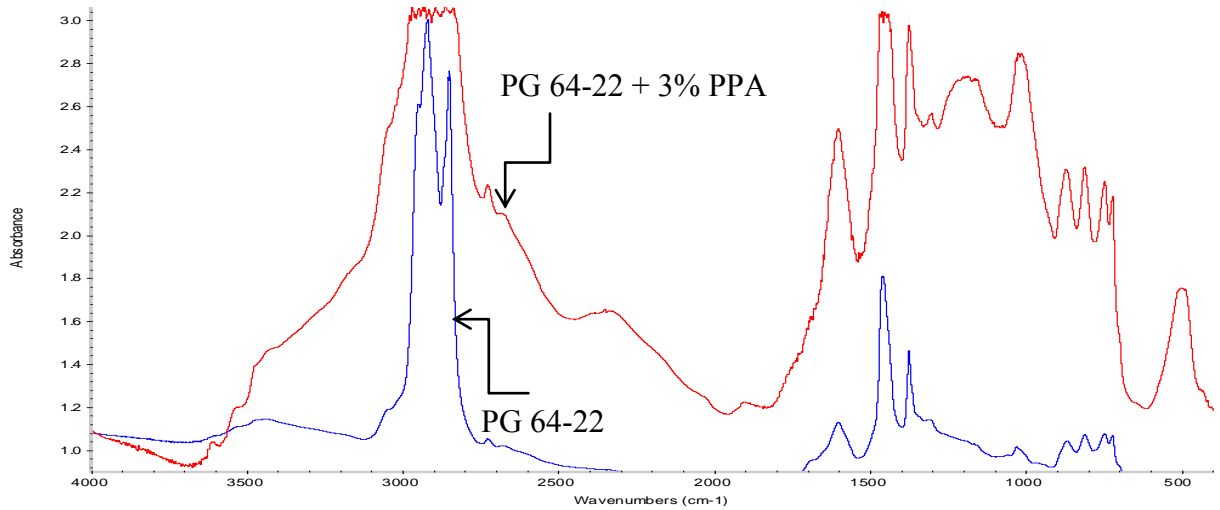


Figure 36: Overlay of FTIR spectra comparing PPA containing and base asphalt binders.

#### 4.4 Aging Characterization by Carbonyl Band

FTIR is a popular technique for aging characterization of asphalt binders. In this research ratio of the area under FTIR spectra in the  $1600\text{ cm}^{-1}$  to  $1700\text{ cm}^{-1}$  (centered around  $1650\text{ cm}^{-1}$ ) was measured and divided by the total area for  $\text{CH}_2 + \text{CH}_3$  (as shown in the following equation) for asphalt binders with and without PPA in the present and absence of SBS polymer. Figure 37 shows a set of aged (Figure 37 (a)) in comparison to a set of unaged samples (Figure 37 (b)). As can be seen the intensity of the carbonyl band at  $1650\text{ cm}^{-1}$  increases as PPA concentration increase for all aged samples. The carbonyl band does not change in the unaged samples irrespective of the PPA concentration (Figure 37 (b)). Following ratio is used to quantify the extent of asphalt oxidation based on the area ratio of the carbonyl band to those of  $\text{CH}_2$  and  $\text{CH}_3$ .

$$I_{\text{CO}} = \frac{\text{Area of the carbonyl band centered around } 1650\text{ cm}^{-1}}{\text{Area of the } \text{CH}_2 \text{ band centered around } 1455\text{ cm}^{-1} + \text{Area of the } \text{CH}_3 \text{ band centered around } 1376\text{ cm}^{-1}}$$

Figure 38 present results of this analysis. Figure 39 shows the difference in Ico (before and after aging taken from figure 38) for all base asphalt samples as well as PPA containing samples with and without polymer.

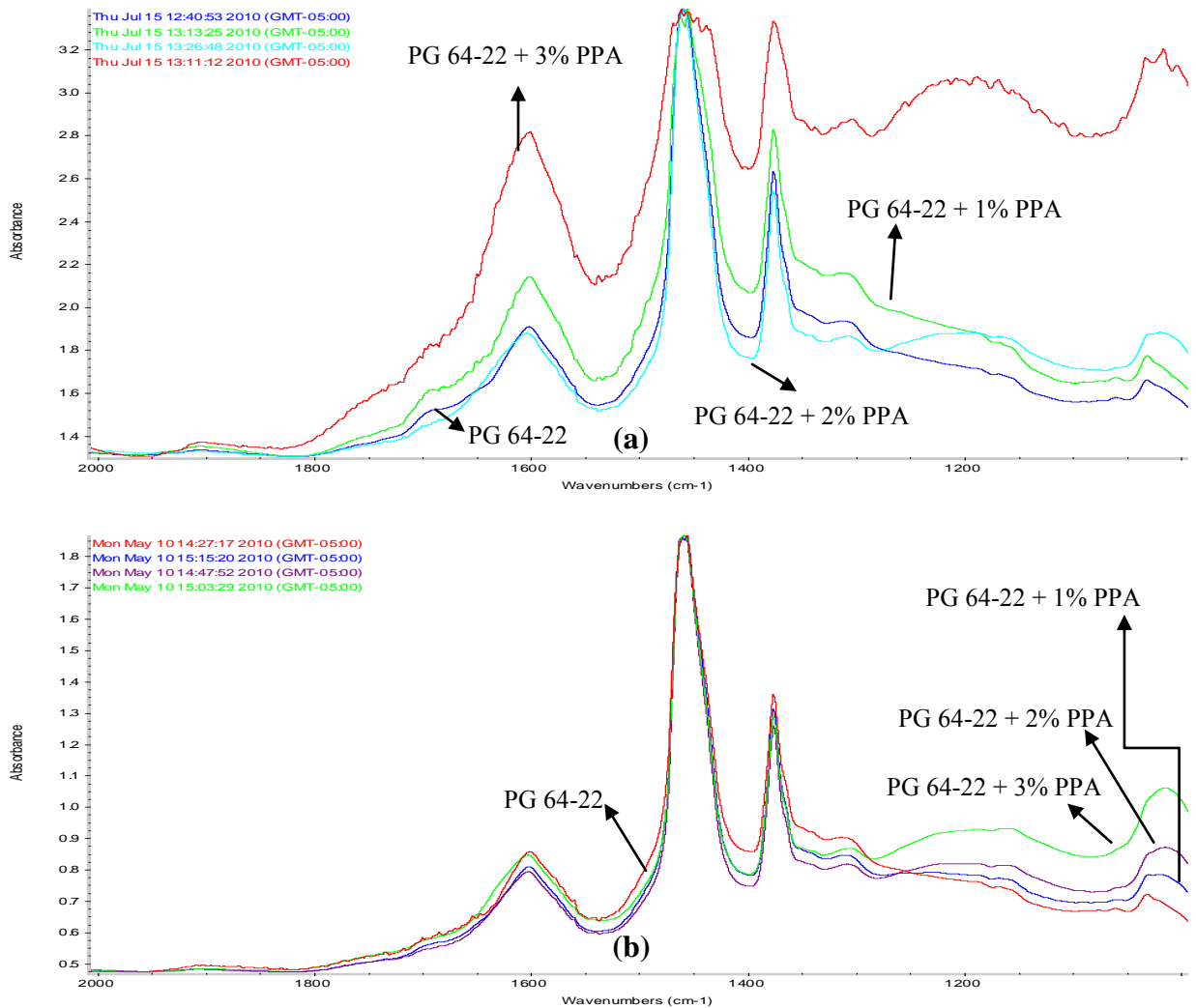


Figure 37: Comparison of FTIR spectra for aged (a) and unaged (b) PPA containing asphalt binders

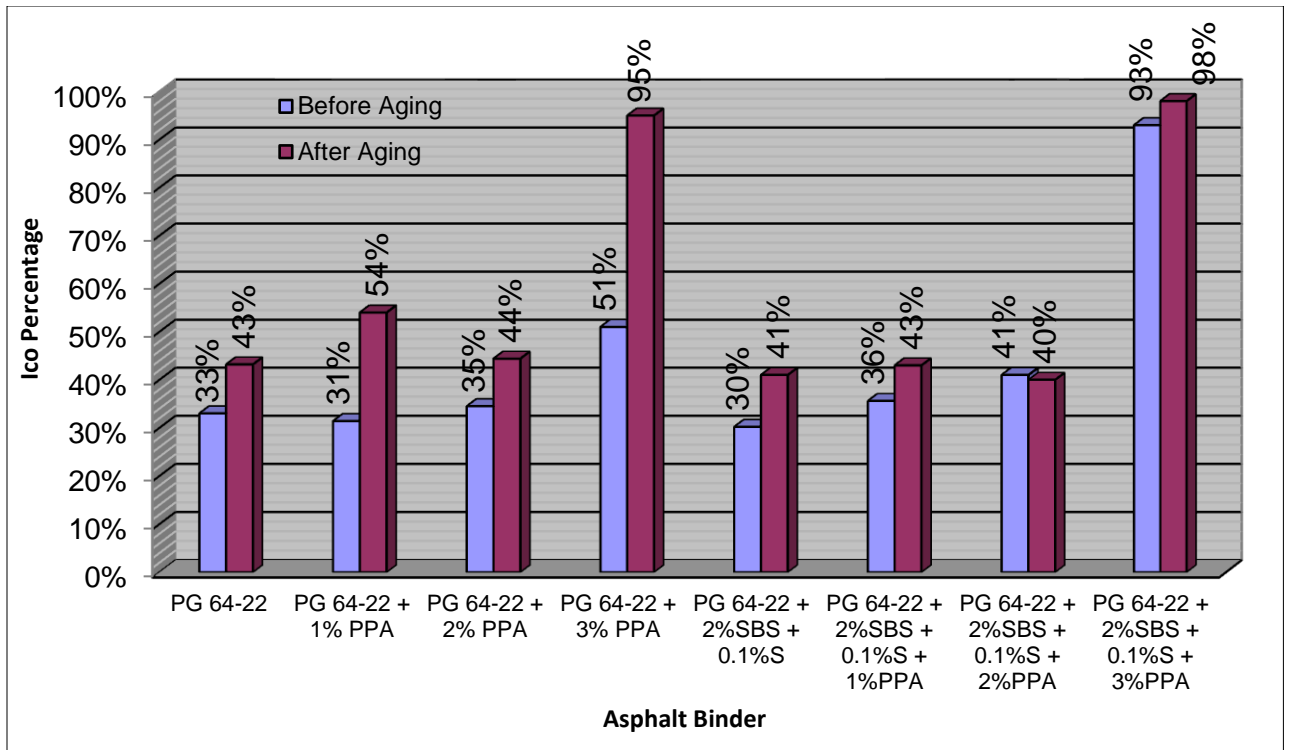


Figure 38: Results of area ratio for carbonyl band to  $\text{CH}_2+\text{CH}_3$  bands for different asphalt samples

When 1-3% PPA is added to the base (PG 64-22) asphalt binder, the increase in Ico percentage (before and after aging) is much higher compared to the binder added with polymer (SBS) and 1-3 % PPA. According to data presented in Figures 38-39, addition of PPA to polymer containing asphalt binder does not increase aging through oxidation of asphalt binder but when polymer is not included in the mix there appears that PPA adversely affects oxidation characteristics of base PG 64-22 asphalt.

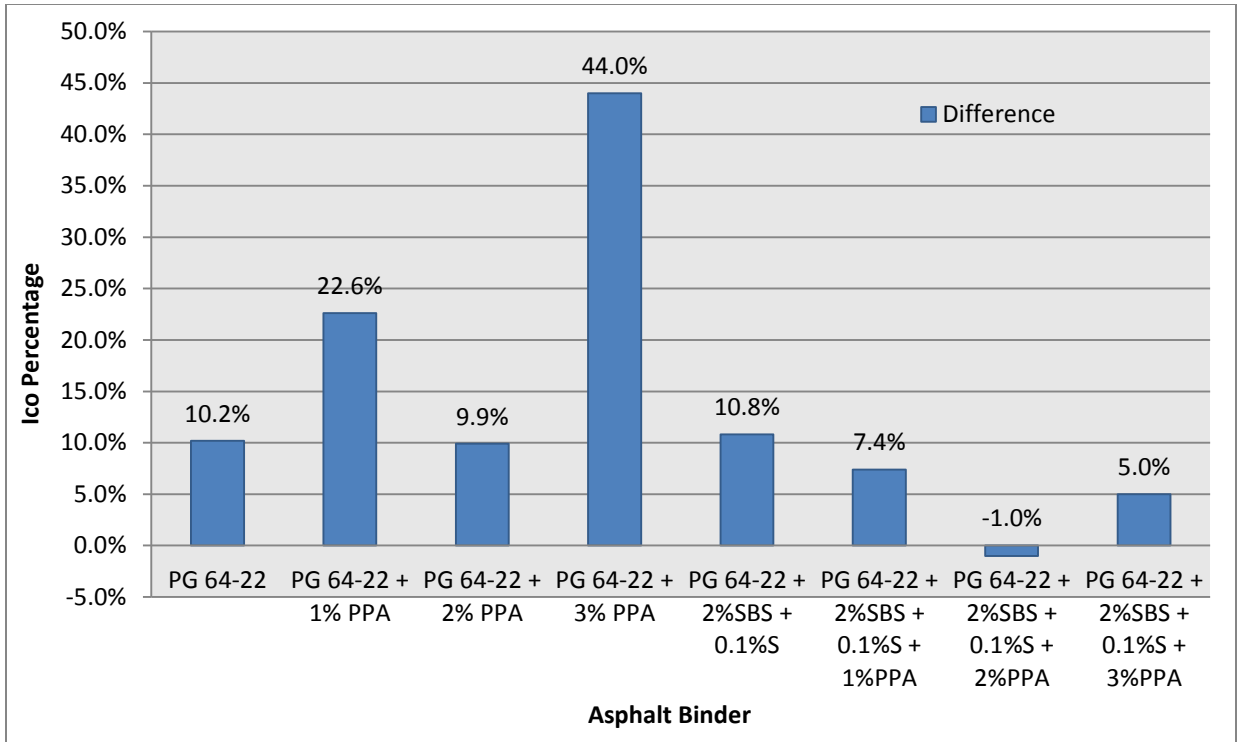


Figure 39: Change in Ico for different asphalt binders due to aging as measured by FTIR.

According to the RTFO results (Figure 39), changes in the carbonyl band show for all samples containing both SBS polymer and PPA the extent of aging is actually less than that of plain PG 64-22 asphalt binder. Plain polymer containing asphalt show nearly similar Ico value (10.8% for PG 64-22 + 2% SBS + 0.1% S compared to 10.2% for PG 64-22 binder). On the other hand, in the absence of SBS polymer addition of 1% PPA and 3% PPA to based asphalt samples showed an increase in Ico percentage by twice and four times respectively. PG 64-22 + 2% SBS + 0.1% S + 2% PPA appears to be acting abnormally as when the sample was prepared, it might have been subjected to heating that would have caused some molecular changes.

The polymer additive, an SBS rubber exhibits a similar set of hydrocarbon bands with the exception of the band at  $966\text{-}968\text{ cm}^{-1}$  belonging to SBS polymer. This band basically proves the presence of the polymer in the asphalt binder; in this case, we used 2% SBS polymer. Figure 40 show that this band is indeed a polymer band. The difference between a PG 64-22 + 2% SBS + 0.1% S and PG 64-22 asphalt binder is shown with the exceptional band at  $966\text{-}968\text{ cm}^{-1}$  circled.

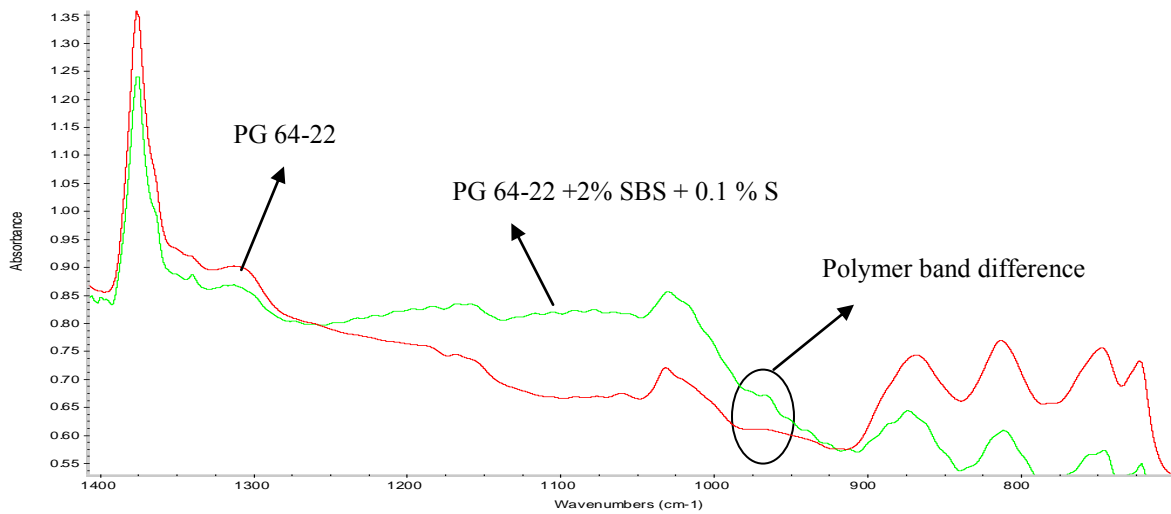


Figure 40: Difference between PG 64-22 + 2% SBS + 0.1% S and PG 64-22 asphalt binder

#### 4.5 Epifluorescence Microscopy

To visualize the asphalt blends, epifluorescence microscopy method was used. The technique applies to samples that can be made to fluorescence, as it is the case with polymer containing asphalt materials. The aged as well as unaged asphalt samples were studied. The data was acquired using a 40x objective on a Zeiss 200M inverted optical microscope with a CSU-10 Yokogawa spinning confocal scanner (confocal microscope laboratory, 2009). The samples were excited at both 405 and 532 nm. The fluorescent

emissions were collected with 450/35 and 585/40 nm (Center/FWHM) filters. Each image was focused for maximum brightness and the exposure was changed when necessary to insure that there was no saturation in the image. The gain of the electron multiplier CCD camera was held constant.

#### 4.5.1 Epifluorescence Microscopy of RTFO Aged Samples

Figure 41 shows image comparison for the base asphalt and samples containing 1-3% PPA. There is not much difference in the appearance of these samples due to the fact that no polymer content is available in any of these samples. In contrast, Figure 42 shows images for samples containing 2% SBS + 0.1% Sulfur. The polymer containing samples do show particles that fluoresce (Figure 42) with very distinct polymer phase bands. The glowing particles in the samples are known to be polymer. By aging, the polymer phase bands have begun to break down and the polymer has begun to spread across the image. The other asphalt binder samples do not show any difference before and after aging in terms of changes in mechanism of interaction between PPA and base asphalt.

The most significant change is with PG 64-22 + 2% SBS + 0.1% S + 3% PPA ((Figures 42(d)). It appears to be acting differently. The polymer has almost spread over the entire image and the initial bands have disappeared as it is aged. These images show the higher the PPA content, the more expanding/elongating the polymer chains.

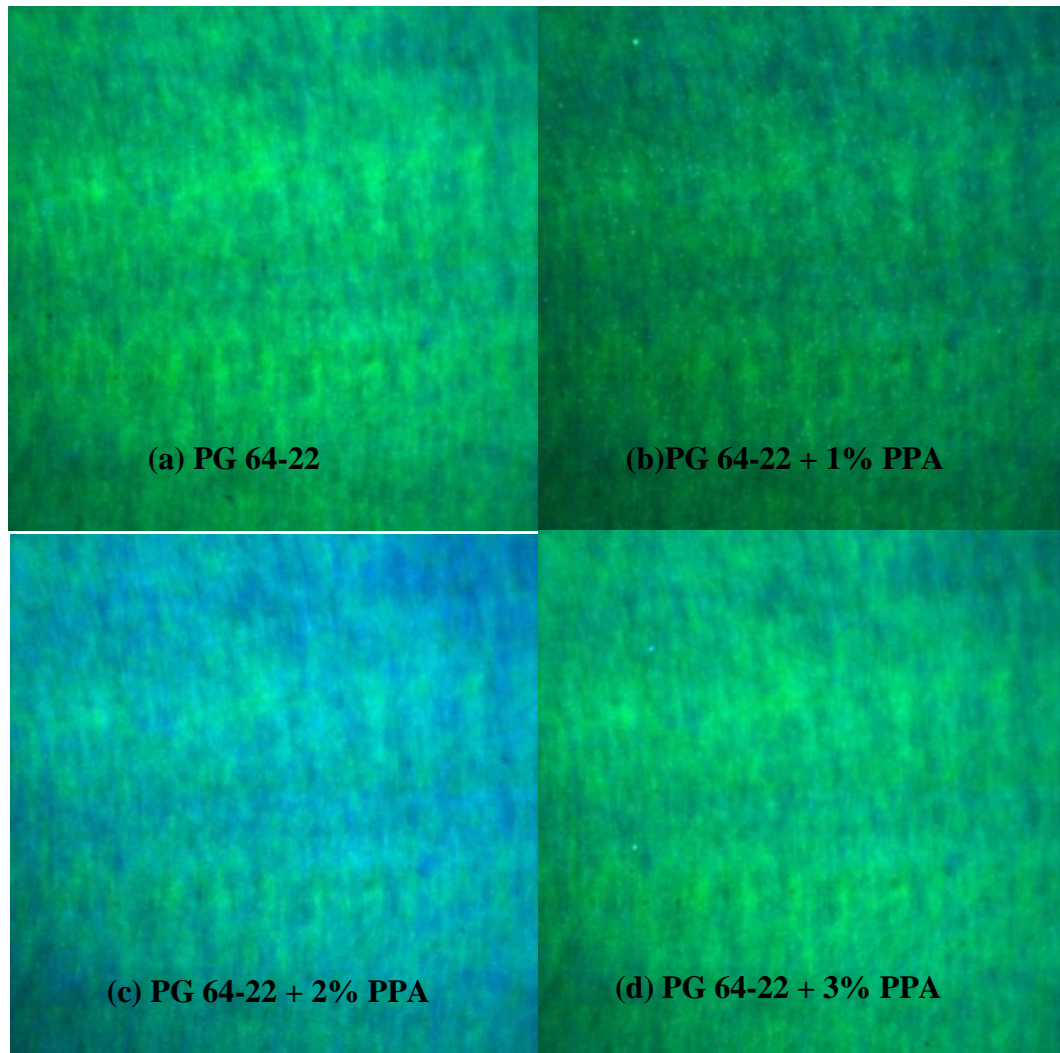


Figure 41: Epifluorescence images of base asphalt (a), 1% PPA added (b), 2% PPA added (c), and 3% PPA added (d).

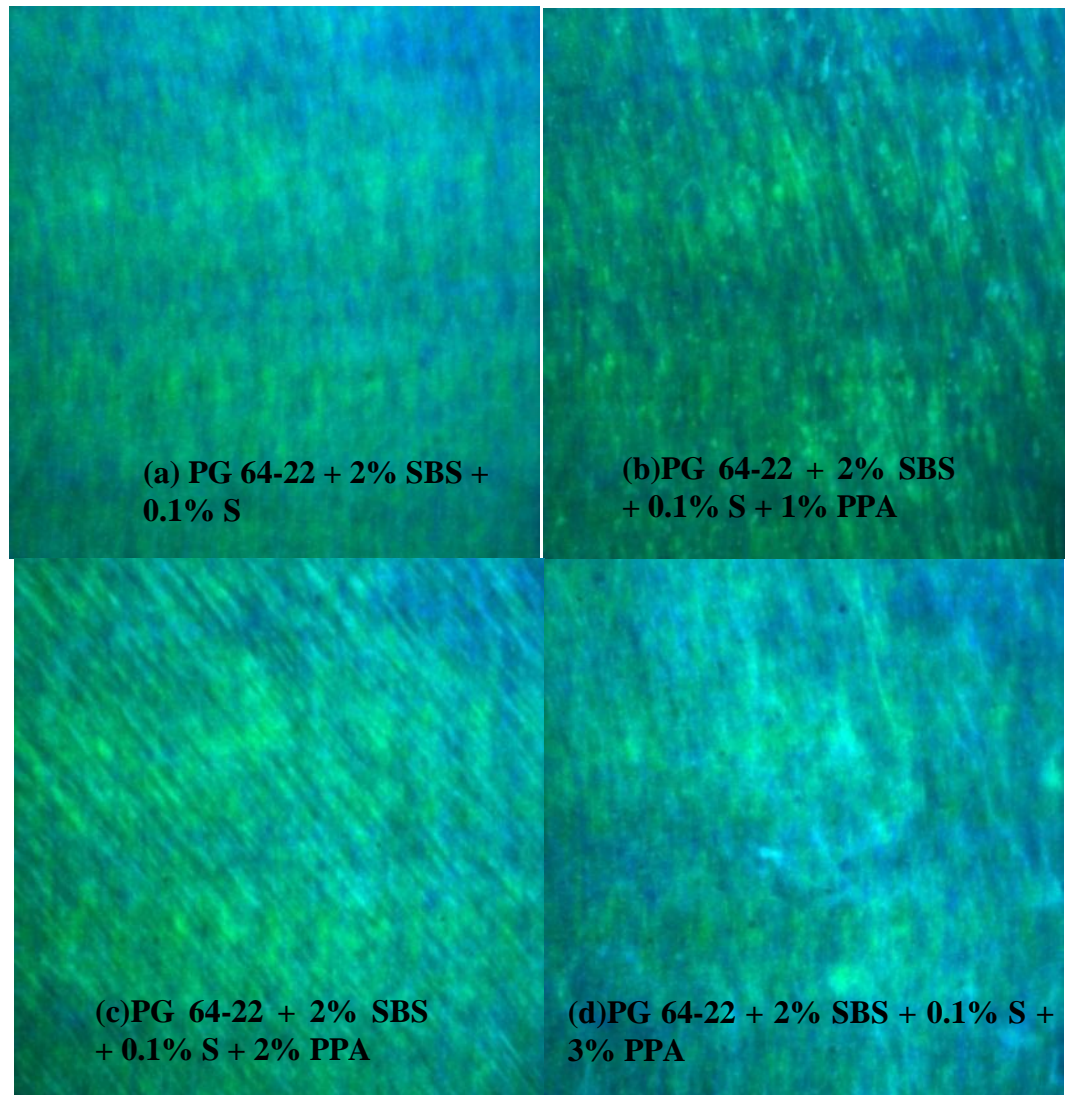


Figure 42: Epifluorescence images of PG 64-22 + 2% SBS + 0.1% S (a), PG 64-22 + 2% SBS + 0.1% S + 1% PPA (b), PG 64-22 + 2% SBS + 0.1% S + 2% PPA (c), and PG 64-22 + 2% SBS + 0.1% S + 3% PPA (d).

#### 4.5.2 Epifluorescence Microscopy of Regular Oven Aged Samples

In order to investigate effects of prolonged heating on both PPA added base asphalt in the presence and absence of SBS polymer constituent, sets of samples were heated in an oven set at 60°C and representative samples were examined under epifluorescence microscope. As anticipated, samples without polymer content did not



show any useful microscopic features to aid identifying interactions between PPA and base asphalt. Therefore no images for those samples are provided here. In contrast, samples containing SBS polymer showed the effects of PPA addition to base asphalt in terms of morphological changes made due to the interaction of these constituents. Figure 43 shows images for base asphalt with only 2%SBS+0.1% S. As can be seen in the image of the unaged sample (Figure 43 (a)) polymer particles are segregated at localized regions. However, upon heating after one week (Figure 43 (b), two weeks (Figure 43 (c)), and after three weeks (Figure 43(d)) fine particles of SBS polymer distributed uniformly throughout the surface of the sample. Such a fine dispersion of the polymeric constituent is desirable from elasticity point of view and prevention of cracking at lower temperatures. These images did not show a long chain formation of the polymers. When 1% PPA (Figures 44) or 2% PPA (Figure 45) was added to the base asphalt +2% SBS+0.1%S and heated for different durations, images corresponding to these samples show similar trend. In these cases, longer heating provided samples with more homogeneous distribution of SBS particles. When concentration of added PPA was elevated to 3%, a distinct pattern for phase distribution was observed as shown in Figure 46. In 3% PPA added sample before aging larger clusters of polymer phase was observed. Upon heating of these large clusters, long chain of polymers (polymer strands) were introduced and with heating continuation these chain shortened and uniformly distributed throughout the entire sample. Image of the two weeks heated sample (Figure 46) shows some clusters are still remained but continuation of heating to 3 weeks formed well defined polymer strands which were uniformly dispersed.

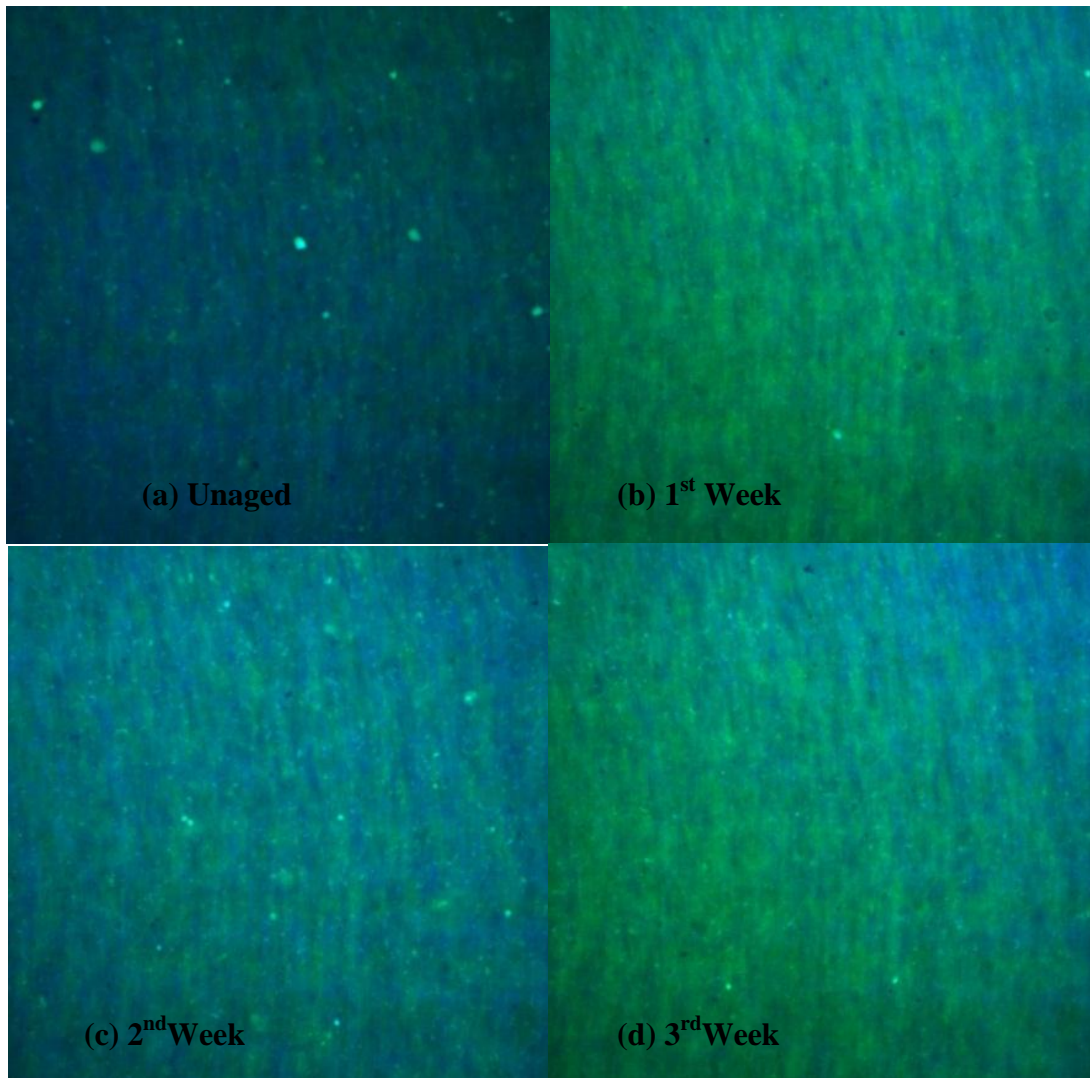


Figure 43: Epifluorescence images of PG 64-22 samples containing 2% SBS + 0.1% S

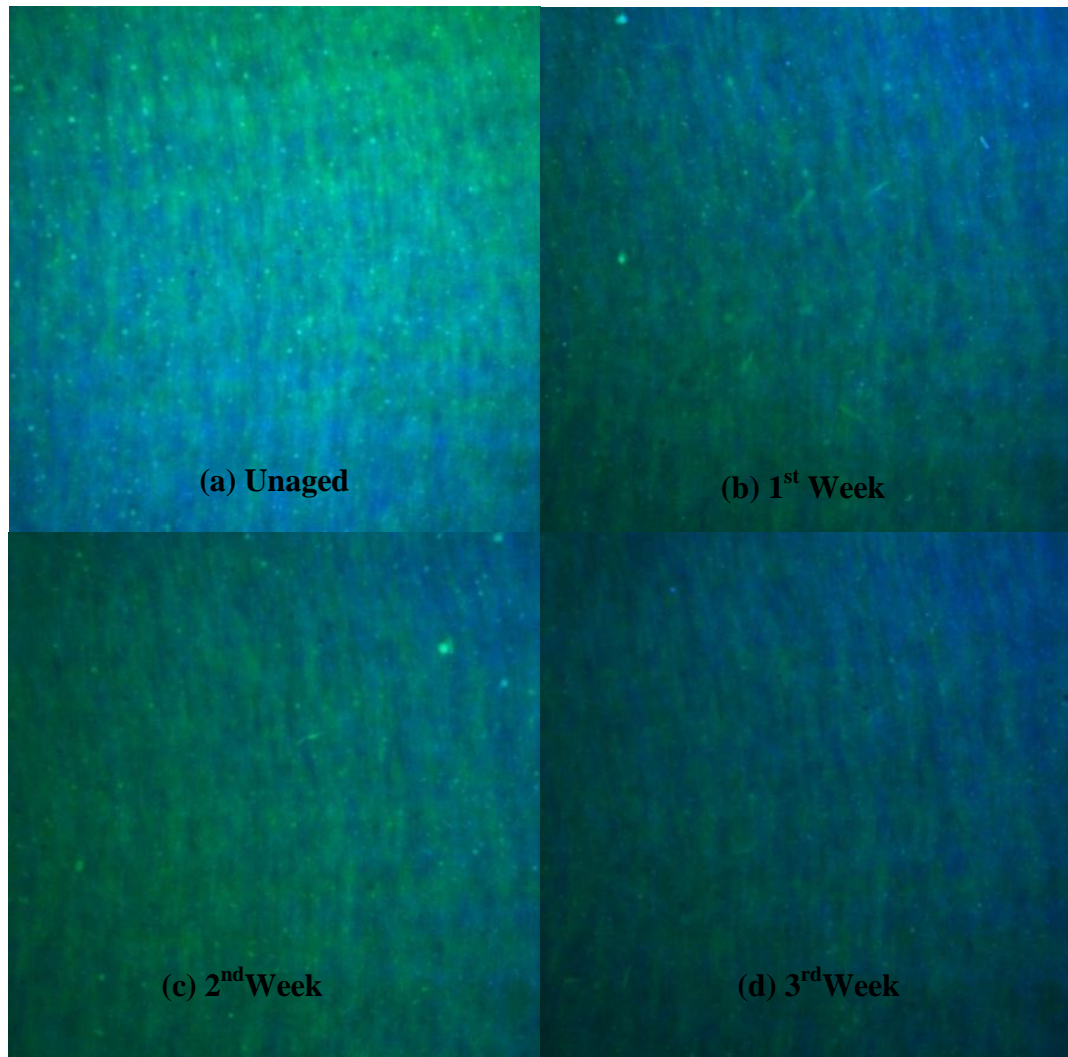


Figure 44: Epifluorescence images of PG 64-22 containing 2% SBS + 0.1% S + 1% PPA

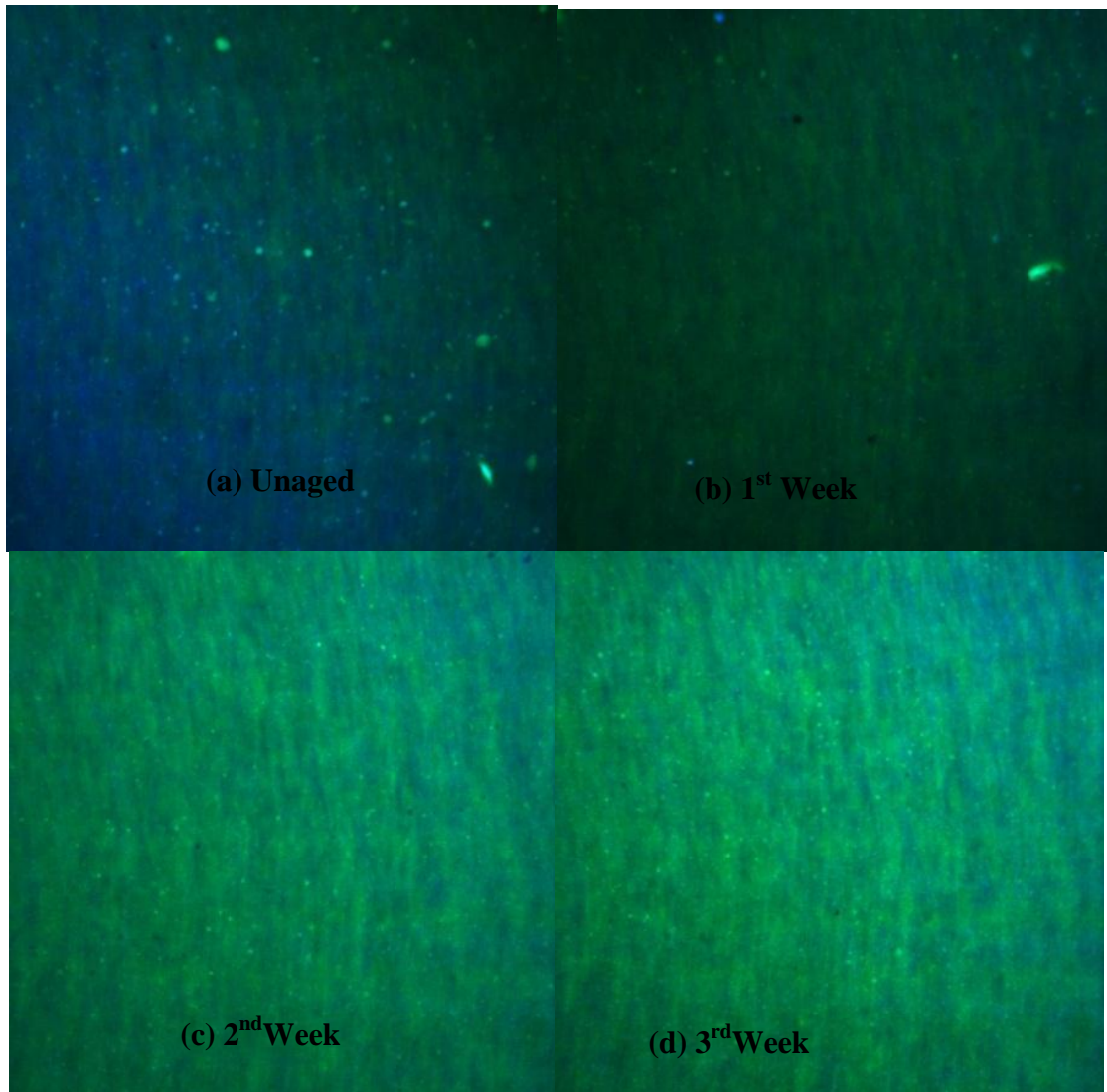


Figure 45: Epifluorescence images of PG 64-22 containing 2% SBS + 0.1% S + 2% PPA

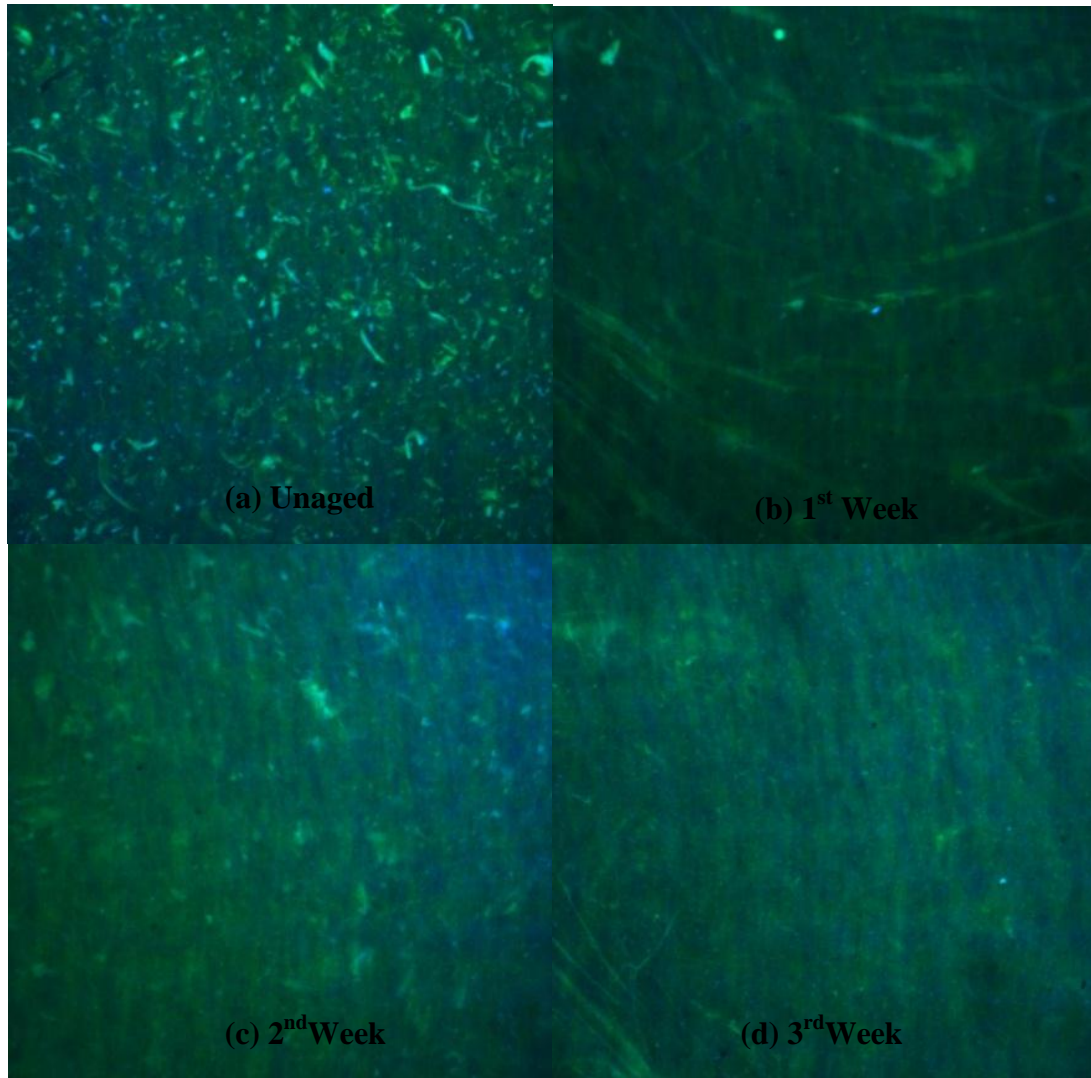


Figure 46: Epifluorescence images of PG 64-22 containing 2% SBS + 0.1% S + 3% PPA

## CHAPTER 5

### CONCLUSION

The aim of this research was to show the advantages of PPA addition to asphalt binders to enhance physical and mechanical properties of modified binders. Addition of PPA increases the stiffness of binders. The increase in stiffness also depends on the type of binder used. The DSR test (quantitative) results support this theory. Also, addition of PPA was expected to actually reduce aging through oxidation of asphalt. This was proved by qualitative analysis done by the FTIR test. Thus, addition of PPA was anticipated to improve pavements performance by reducing both fatigue cracking and low temperature cracking.

In conclusion, the results obtained from this research led to the following:

- PPA addition to PG 64-22 does increase the stiffness of asphalt binders (with and without polymer content).
- The extent of the stiffening effect depends linearly on PPA concentration in the 1-3% range for PG 64-22 binder.
- PPA addition to PG 64-22 lowered  $\delta$  for both polymer and non-polymer containing asphalt. Reduction of  $\delta$  was more pronounced in polymer containing asphalt suggesting a synergistic effect of PPA and polymer on enhancement of asphalt mechanical properties (stiffness and elasticity) at 60°C.

- As anticipated, increase in  $G^*/\sin \delta$  resulted in decrease in percentage strain in all samples indicating as stiffness of asphalt increased, its elasticity decreased.
- Based on Ico measurements using FTIR, addition of PPA to PG 64-22 negatively affects aging characteristics of non-polymer containing asphalt severely, however, polymer containing PG-64-22 asphalt showed strong aging resistance enhancement by PPA addition. FTIR results further indicated effects of PPA addition to the binder on  $\text{CH}_2/\text{CH}_3$  ratio.
- Epifluorescence microscopy showed polymer strand formation from polymer clusters and uniform polymer strand distribution after prolonged heating (3 weeks at  $60^\circ\text{C}$ ).

## REFERENCES

AASHTO T 321, Standard Method of Test for Determining the Fatigue Life of Compacted Hot-Mix Asphalt (HMA) Subjected to Repeated Flexural Bending, AASHTO, Washington D.C., 2008.

Alexander, S. H. “Method of treating asphalt”, US Patent 3,751,278, 1973.

Asphalt Institute, [http://www.asphaltinstitute.org/upload/Spring\\_04\\_AI\\_Lab\\_Corner.pdf](http://www.asphaltinstitute.org/upload/Spring_04_AI_Lab_Corner.pdf) (viewed 10/15/10).

Baumgardner G. L., “Polyphosphoric Acid Modified Asphalt Binders –Industry Perspective; Usage, Why, How”, Paragon Technical Services, Inc., April 2009, <https://engineering.purdue.edu/NCSC/PPA%20Workshop/2009/index.html> (viewed 09/09/10).

Bell, C.A., Y. Abwahab, M.E. Cristi, and D. Sosnovske, “Selection of Laboratory Aging Procedures for Asphalt-Aggregate Mixtures”. Report SHRP-A-38. Strategic Highway Research Program, National Research Council, Washington, DC, pp. 1-10, 1994.

Bennert, T., “Polyphosphoric Acid in Combination with Styrene-Butadiene-Styrene Block Copolymer: Laboratory Mixture Evaluation”, Rutgers University: Center for Advanced Infrastructure and Transportation (CAIT), April 2009, <https://engineering.purdue.edu/NCSC/PPA%20Workshop/2009/index.html> (viewed 09/09/10).

Brule, B., Planche, J.P., King, G., Claudy, P., and Letoffe, J.M., “Characterization of Paving Asphalts by Differential Scanning Calorimetry”, Fuel Science & Technology International, 1991, 9, pp. 71-92.

Buncher, M., “Polyphosphoric Acid Modification of Asphalt”, 2009, <https://engineering.purdue.edu/NCSC/PPA%20Workshop/2009/index.html> (viewed 09/09/10).

Burke R.E., and C. H. Whitacre, “Manufacture of Improved Asphalts”, U.S. Patent, no. 2,179,208, 1939.

Arika, Caleb N., Canelon, Dario J., Nieber, John L., “Subsurface Drainage Manual for Pavements in Minnesota”, Minnesota Department of Transportation, 2009, pp. 63, <http://www.lrrb.org/PDF/200917.pdf>



- Chen, J. S., and Huang, L. S., "Developing an aging model to evaluate engineering properties of asphalt paving binders", *Materials and Structures Constructions*, vol. 33, pp. 559-565, Nov 2000.
- C.H. Domke, R.R. Davison, and C.J. Glover, Effect of Oxygen Pressure on Asphalt Oxidation Kinetics. *Ind. Eng. Chem. Res.* 2000, 39, 592.
- Clayton, T., and Peterson, T., "PG Binders, Taking the mystery out of the numbers", Colorado Asphalt Pavement Association (CAPA), v08, no. 2, pp. 1-4. 2009.
- Confocal Microscope Laboratory, Department of Biological Sciences, University of North Texas, Epifluorescence Microscopy, Jan 2009,  
<http://www.biol.unt.edu/Confocal/Confocal%20Microscope.html> (viewed 06/11/10).
- Controls Testing equipment for the Construction Industry, Rolling Thin Film Oven (RTFO), 2007,  
[http://www.controls.it/products.php?code=144&page=Resistance\\_to\\_hardening-ageing&product=432&product\\_name=Rolling\\_Thin-Film\\_Oven\\_%28RTFOT\\_Method%29&language=1](http://www.controls.it/products.php?code=144&page=Resistance_to_hardening-ageing&product=432&product_name=Rolling_Thin-Film_Oven_%28RTFOT_Method%29&language=1) (viewed 05/20/10).
- Daranga, C., "Characterization of aged polymer modified asphalt cements for recycling purposes", Ph. D. Dissertation, Department of Chemistry, Louisiana State University, Baton Rouge, LA., pp. 2-80, 2005.
- Daranga, C., Clopotel, C., Mofolasayo, A., and Bahia, H., "Storage Stability and Effect of Mineral Surface on Polyphosphoric Acid (PPA) Modified Asphalt Binders," *Presented during Poster Session*, 88th Annual Meeting of the Transportation Research Board; Washington, D.C., pp. 2-11, 2009.
- D'Angelo, J., "PPA and Binder Modification", Office of Pavement Technology, April 2009, <https://engineering.purdue.edu/NCSC/PPA%20Workshop/2009/index.html> (viewed 09/09/10).
- De Filippis, P., C. Giavarini and M. Scarsella, "Improving the ageing resistance of straight-run bitumens by addition of phosphorus compounds", *Fuel*, v74, no. 6, 836-841, 1995.
- Donald W., Lynn E., Susan K., "Paser Asphalt Roads Manual", Wisconsin Transportation Information Center, Pavement Surface Evaluation and Rating, pp. 3-28, 1987, 1989, 2002.
- Feng Zhang, Jianying Yu, "The research for high-performance SBR compound modified asphalt", *Construction and Building Materials*, v24, Issue 3, pp. 410-418, March 2010.

Freemantle, Ml., What's that Stuff?, Chemical and Engineering (C&E) News, v77, no. 47 pp. 81, November 1999.

Gecan, Dynamic Shear Rheometer (DSR), 2007,  
[http://www.gecan.ca/photo\\_gallery/photo\\_gallery.aspx](http://www.gecan.ca/photo_gallery/photo_gallery.aspx) (viewed 10/23/10).

Glover, I.C., Department of Chemistry, Louisiana State University, "Wet and Dry Aging of Polymer-Asphalt Blends: Chemistry and Performance", pp. 1, 2007.

Herrington, Philip R., George F. A. Ball, Temperature dependence of asphalt oxidation mechanism, Fuel, v75, Issue 9, July 1996, pp. 1129-1131.

Huang, S.C., Turner, T.F., Miknis, F.P., Thomas, K.P., "Long-term aging characteristics of polyphosphoric acid modified asphalts", Transportation Research Record: Journal of the Transportation Research Board, Washington D.C., v2051, October 2008.

Kearney, E.J., and Blades, C., "Asphalt Paving Principles", Cornell Local Roads Program, New York LTAP Center , 3, pp. 34-42, March 2004.

Khattak, M. J., and Baladi, G. Y., "Engineering Properties of Polymer-Modified Asphalt Mixtures", Transportation Research Record 1638, National Research Council, Washington, D.C., 1998.

Kraton,  
[http://www.kraton.com/Applications/Bitumen\\_Modification/Roads/Pavement\\_Distress/Fatigue\\_Cracking/](http://www.kraton.com/Applications/Bitumen_Modification/Roads/Pavement_Distress/Fatigue_Cracking/) (viewed 10/15/10).

Lamontagne J., Dumas P., Mouillet V., Kister J., "Comparison by Fourier transform infrared (FTIR) spectroscopy of different ageing techniques: application to road bitumens", Fuel 2001, 80, pp. 483-488.

Lau, C.K., Lunsford, K.M., Glover, C.J., Davison, R.R., Bullin, J.A., Reaction Rates and Hardening Susceptibilities as Determined from POV Aging of Asphalts. Trans. Res. Rec. 1992, 50, 1342.

Harwood, Laurence M., Moody, Christopher J., "Experimental organic chemistry: Principles and Practice" (Illustrated ed.). Wiley-Blackwell. pp. 292, 1989.

Lee, D.Y., Huang, R.J. Weathering of Asphalts As Characterized by Infrared Multiple Internal Reflection Spectra. Chem. 1973, 46, 2242.

Le Guern, M., Chailleux, E., Farcas, F., Dreessen, S., Mabile, I., "Physico-chemical analysis of five hard bitumens: Identification of chemical species and molecular

organization before and after artificial aging”, Fuel, Volume 89, Issue 11, pp. 3330-3339, Nov 2010.

Martin, K.L. Davison, R.R. Glover, C.J. Bullin, J. A., Asphalt Aging in Texas Roads and Test Sections. Trans. Res. Rec.1990, 1269, 9.

Masson J-F, Collins P., Woods J.R., Bundalo-Perc S., Margeson, J. “Chemistry and effects of polyphosphoric acid on the microstructure, molecular mass, glass transition temperatures and performance grades of asphalts”, Journal of the Association Asphalt Paving Technologists (AAPT), 2009, 78, pp. 403–430.

Masson J-F., Collins, P., “FTIR study of the reaction of polyphosphoric acid and model bitumen sulfur compounds”, Energy Fuels 2009, 23(1), pp. 440–442.

National Center for Asphalt Technology (NCAT), 1999. Welcome to NCAT online. <http://www.eng.auburn.edu/research/centers/ncat/about/index.html> (viewed 05/15/10).

Oft, W.P.V. “Durability of Asphalt: It’s Aging in the Dark”, Industrial and Engineering Chemistry, 48(7), 6-15, 1956.

Partl, M. N., Gubler, R., Poulidakos, L.D., and Sokolov, K., “Innovations in testing of Bituminous Pavement Materials”, In *5th International Symposium on Binder Rheology and Pavement Performance*, Baltimore, MD, 2004.

Pavement Interactive, <http://pavementinteractive.org/index.php?title=DSR> (viewed 10/14/2010).

Peterson, J.C., Branthaver, J.F., Robertson, R.E., Harnsberger, P.M., Duvall, J.J., Ensley, E.K., Effects of Physicochemical Factors on Asphalt Oxidation Kinetics. Trans. Res. Rec. 1993, 1391, 1.

Roughneck Chronicles, <http://www.roughneckchronicles.com/Refining/asphaltrefining.html> (viewed 10/15/10).

Sargand, S.M., Kim, S.S., “Performance evaluation of polymer modified and unmodified Superpave mixes”, Second International Symposium on Maintenance and Rehabilitation of Pavements and Technological Control, Auburn, AL, 2001.

Reubush, S. D., “Effects of storage on the linear viscoelastic response of polymer-modified asphalt at intermediate to high temperatures”, Virginia Polytechnic Institute and State University, Master of Science in Civil Engineering, pp.17, 1999.

Sisko, A. W. a. B. L. C., "The Rheological Properties of Asphalts in Relation to Durability and Pavement Performance", Proceedings of Association of Asphalt Paving Technologists, 1968, 37, pp. 28-39.

Stacey, Ed., Blachford, L., Cengage, G., "Asphalt Cement - How Products are Made", 2002. eNotes.com. 2006. (viewed 10/12/10)  
<<http://www.enotes.com/how-products-encyclopedia/asphalt-cement>>

Arnold, Terry S., Needham, Susan P., and Youtcheff, J. "The Use of Phosphoric Acid as a Modifier for Hot Mix Asphalt", pp. 2-15, November 2008.

Thermo Nicolet Avatar 370 DTGS, Department of Engineering Technology, University of North Texas, 2010.